Table 7. Changes in alveolar bone height at 36 weeks

		Group P (n = 19)	Group L (n = 19)	Group M (n = 19)	Group H (n = 17)
rate of increase (%)	Mean (SD)	23.92 (27.52)	20.19 (38.09)	29.39 (37.71)	58.62 (46.74)
	Mean differences		−3.73	5.47	34.7
	from Group P (95%CI)		(−28.22–20.77)	(−19.02–29.97)	(9.50–59.91)
	Adjusted p value*		0.981	0.945	0.021
millimeter increase	Mean (SD)	0.95 (1.26)	0.54 (1.26)	1.06 (1.16)	1.85 (1.75)
	Mean differences		−0.41	0.11	0.90
	from Group P (95%CI)		(−1.24–0.42)	(−0.69–0.91)	(−0.13–1.92)
	Adjusted p value*		0.678	0.990	0.132

*Adjusted for multiple comparisons based on Dunnett's test.

doi:10.1371/journal.pone.0002611.t007

administration of the investigational drug and the frequency of any adverse events (see Table S4 of supporting items). Although some adverse events did emerge in patients administered FGF-2, no relationship was recognizable between frequency of these events and FGF-2 concentrations. In addition, the same adverse events also emerged in the placebo group. Those effects are therefore not specific to groups administered FGF-2 and do not appear attributable to the drugs administered. Another reason why we consider that FGF-2 administered locally to periodontal tissue seldom travels through the whole body to create adverse drug reactions is that the protein was undetectable in serum after drug administration. Furthermore, no patients displayed increased levels of anti-FGF-2 antibody after administration, suggesting that FGF-2 is free from antibody production, an adverse drug reaction often seen with other proteinaceous agents. In short, none of the results of this particular clinical trial suggest any clinical problems concerning the safety of administering FGF-2 to patients with periodontitis. One more piece of evidence supporting the high safety of FGF-2 applied locally to periodontal tissue is that this therapy has already been used for more than 5 years as a remedy for intractable ulcers (Fiblast spray).

Periodontitis shortens the life of teeth and can thus reduce QOL in middle-aged to elderly individuals [4]. To maintain and promote oral health, new therapies must be established for safe and efficient regeneration of periodontal tissue. Cytokine therapy has thus been winning attention for the last decade [6–15,19]. However, few double-blinded clinical trials have used multiple facilities in compliance with GCP guidelines to confirm the efficacy of a single cytokine alone as a stimulator of periodontal tissue regeneration. In the present clinical trial, 0.3% FGF-2 improved CAL by about 2 mm at 36 weeks from base. And more importantly, rate of increase in bone height observed in close proximity to the dental root was significantly improved in 0.3% FGF-2 treatment group compared to placebo group at 36 weeks. These findings were clinically interpreted that some efficacy could be expected from FGF-2 in stimulating regeneration of periodontal tissue. Thus, we concluded in this study that FGF-2 therapy can be efficacious in regenerating periodontal tissue. However, an important limitation of this study is the small sample size of the trial. This trial is still preliminary, and several trials need to be performed before FGF-2 drug can be placed on the market. In future, we plan to clarify the efficacy of FGF-2 drug, determine the optimal dose for clinical use and confirm in more detail the safety of FGF-2 in a large Phase II study. And then Phase III will be performed to confirm the efficacy and safety of the invitational drug.

(This clinical trial was conducted at the request of Kaken Pharmaceutical Co., Ltd.)

Supporting Information

Checklist S1 CONSORT Checklist.
Found at: doi:10.1371/journal.pone.0002611.s001 (0.04 MB DOC)

Protocol S1 Trial Protocol.
Found at: doi:10.1371/journal.pone.0002611.s002 (0.11 MB DOC)

Table 8. Clinical Attachment Level (CAL) regained at 36 weeks

		Group P (n = 19)	Group L (n = 19)	Group M (n = 19)	Group H (n = 17)
mm of CAL regained	Mean (SD)	2.63 (1.54)	2.00 (2.08)	2.02 (2.08)	2.18 (1.33)
	Mean differences		−0.63	−0.61	−0.46
	From Group P (95%CI)		(−1.84–0.57)	(−1.81–0.60)	(−1.43–0.53)
	Adjusted p value*		0.573	0.604	0.792
% of CAL regained	Mean (SD)	29.65 (17.00)	24.03 (25.31)	24.20 (28.27)	29.69 (23.14)
	Mean differences		−5.62	−5.45	0.04
	from Group P (95%CI)		(−19.81–8.60)	(−20.79–9.90)	(−13.61–13.70)
	Adjusted p value*		0.810	0.823	1.000

*Adjusted for multiple comparisons based on Dunnett's test.

doi:10.1371/journal.pone.0002611.t008

Table S1 Clinical inspections.
Found at: doi:10.1371/journal.pone.0002611.s003 (0.03 MB DOC)

Table S2 Changes in periodontal tissue. Mean and standard deviations are shown. *Data at 36 weeks were missing for 1 patient in Group M.
Found at: doi:10.1371/journal.pone.0002611.s004 (0.07 MB DOC)

Table S3 Changes in periodontal tissue. All of data at 36 weeks were missing for 1 patient in Group M. Data for MO were missing at 12 weeks for each patient in Groups P and H, at 24 weeks in Group H and at 36 weeks in Group H.
Found at: doi:10.1371/journal.pone.0002611.s005 (0.07 MB DOC)

Table S4 List of adverse drug reactions. *Pains experienced by 1 patient in Group M required therapy, and the patient began to experience pain at the surgical site starting 8 days after administration that resolved 35 days after administration with the use of drugs such as cefcapene pivoxil hydrochloride, lysozyme hydrochloride, rebamipide and loxoprofen sodium.

Found at: doi:10.1371/journal.pone.0002611.s006 (0.04 MB DOC)

Acknowledgments

We wish to thank all the investigators who participated and most of all the patients for their important contributions to the study. We would also like to thank Katsuyasu Eguchi, Toshiyuki Yorozuya, Hayuru Koizumi, Shinya Horimoto, Motoki Akamatsu (Kaken Pharmaceutical Co., Ltd.) and Takenori Nozaki (Osaka University Dental Hospital) for their critical support of this study.

Author Contributions

Conceived and designed the experiments: SM MK MW. Performed the experiments: MK KN YK TF HS MF TN TS YI ST HK MN JK TN TH KM YH YI TH. Analyzed the data: SM MK MW. Wrote the paper: SM MK KN TF HS MF TN TS YI ST HK MN JK TN TH KM YH YI TH MW. Other: Measured the X-ray film data: TF TS. Participated in interpretation of the results: TF EI MO TS. Confirmed safety of all patients throughout the study period: MO EI.

References

1. Nishihara T, Koseki T (2004) Microbial etiology of periodontitis. Periodontology 2000 36: 14–26.
2. Socransky SS, Haffajee AD (2002) Dental biofilms: difficult therapeutic targets. Periodontology 2000 28(1): 12–55.
3. Ezzo PJ, Cutler CW (2003) Microorganisms as risk indicators for periodontal disease. Periodontology 2000 32(1): 24–35.
4. Kinane DF (2001) Causation and pathogenesis of periodontal disease. Periodontology 2000 25(1): 8–20.
5. Seo BM, Miura M, Gronthos S, Bartold PM, Batouli S, et al. (2004) Investigation of multipotent postnatal stem cells from human periodontal ligament. Lancet 364: 149–155.
6. Lynch SE, Williams RC, Polson AM, Howell TH, Reddy MS, et al. (1989) A combination of platelet-derived and insulin-like growth factors enhances periodontal regeneration. J Clin Periodontol 16: 545–548.
7. Kinoshita A, Oda S, Takahashi K, Yokota S, Ishikawa I (1997) Periodontal regeneration by application of recombinant human bone morphogenetic protein-2 to horizontal circumferential defects created by experimental periodontitis in beagle dogs. J Periodontol 68: 103–109.
8. Sigurdsson TJ, Lee MB, Kubota K, Turek TJ, Wozney JM, et al. (1995) Periodontal repair in dogs: recombinant human bone morphogenetic protein-2 significantly enhances periodontal regeneration. J Periodontol 66: 131–138.
9. Mohammed S, Pack AR, Kankaanranta TH (1998) The effect of transforming growth factor beta one (TGF-beta 1) on wound healing, with or without barrier membranes, in a Class II furcation defect in sheep. J Periodontal Res 33: 335–344.
10. Giannobile WV, Ryan S, Shih MS, Su DL, Kaplan PL, et al. (1998) Recombinant human osteogenic protein-1 (OP-1) stimulates periodontal wound healing in class III furcation defects. J Periodontol 69: 129–137.
11. Takeda K, Shiba H, Mizuno N, Hasegawa N, Mouri Y, et al. (2005) Brain-derived neurotrophic factor enhances periodontal tissue regeneration. Tissue Eng 11: 1618–1629.
12. Nevins M, Giannobile WV, McGuire MK, Kao RT, Mellonig JT, et al. (2005) Platelet-derived growth factor stimulates bone fill and rate of attachment level gain: results of a large multicenter randomized controlled trial. J Periodontol 76: 2205–2215.
13. Murakami S, Takayama S, Ikezawa K, Shimabukuro Y, Kitamura M, et al. (1999) Regeneration of periodontal tissues by basic fibroblast growth factor. J Periodont Res 34: 425–430.
14. Takayama S, Murakami S, Shimabukuro Y, Kitamura M, Okada H (2001) Periodontal regeneration by FGF-2 (bFGF) in primate models. J Dent Res 80: 2075–2079.
15. Murakami S, Takayama S, Kitamura M, Shimabukuro Y, Yanagi K, et al. (2003) Recombinant human basic fibroblast growth factor (bFGF) stimulates periodontal regeneration in class II furcation defects created in beagle dogs. J Periodont Res 38: 97–103.
16. Löe H, Silness J (1963) Periodontal disease in pregnancy. I. Prevalence and severity. Acta Odontol Scand 21: 533–551.
17. Miller SC (1950) Textbook of Periodontia, 3rd ed. Philadelphia and Toronto: The Blakiston Co.
18. Silness J, Löe H (1964) Periodontal disease in pregnancy. II. Correlation between oral hygiene and periodontal condition. Acta Odontol Scand 22: 121–135.
19. Howell TH, Fiorellini JP, Paquette DW, Offenbacher S, Giannobile WV, et al. (1997) A phase I/II clinical trial to evaluate a combination of recombinant human platelet-derived growth factor-BB and recombinant human insulin-like growth factor-I in patients with periodontal disease. J Periodontol 68: 1186–1193.
20. Ledoux D, Gannoun-Zaki L, Barritault D (1991) Interactions of FGFs with target cells. Prog Growth Factor Res 4: 107–120.
21. Takayama S, Yoshida J, Hirano H, Okada H, Murakami S (1997) Effects of basic fibroblast growth factor on human gingival epithelial cells. J Periodont Res 32: 667–675.
22. Gilman NS, Isik FF, Heimbach DM, Gordon D (1994) Basic fibroblast growth factor in the early human burn wound. J Surg Res 56: 226–234.
23. Yu W, Naim JO, Lanzafame RJ (1994) Expression of growth factors in early wound healing in rat skin. Lasers Surg Med 15: 281–289.
24. Richard JL, Parer-Richard C, Daures JP, Clouet S, Vannereau D, et al. (1995) Effect of topical basic fibroblast growth factor on the healing of chronic diabetic neuropathic ulcer of the foot. A pilot, randomized, double-blind, placebo-controlled study. Diabetes Care 18: 64–69.
25. Okumura M, Okuda T, Nakamura T, Yajima M (1986) Acceleration of wound healing in diabetic mice by basic fibroblast growth factor. Biol Pharm Bull 19: 530–535.
26. Kilic AR, Eleoglu E, Yilmaz S (1997) Guided tissue regeneration in conjunction with hydroxyapatite-collagen grafts for intrabony defects. A clinical and radiological evaluation. J Clin Periodontol 24: 372–383.
27. Zetterstrom O, Andersson G, Eriksson L, Fredriksson A, Friskopp J, et al. (1997) Clinical safety of enamel matrix derivative (EMDOGAIN) in the treatment of periodontal defects. J Clin Periodontol 24: 697–704.
28. Egelberg J (1987) Regeneration and repair of periodontal tissues. J Periodont Res 22: 233–242.
29. Caton J, Zander HA (1976) Osseous repair of an intrabony pocket without new attachment of connective tissue. J Clin Periodontol 3: 51–58.
30. Wikesjo UM, Nilveus R (1991) Periodontal repair in dogs. Healing patterns in large circumferential periodontal defects. J Clin Periodontol 18: 49–59.
31. Bowers GM, Schallhorn RG, Mellonig JT (1982) Histologic evaluation of new attachment in human intrabony defects. A literature review. J Periodontol 53: 509–514.
32. Shimono M, Ishikawa T, Ishikawa H, Matsuzaki H, Hashimoto S, et al. (2003) Regulatory mechanisms of periodontal regeneration. Microsc Res Tech 60: 491–502.
33. Lekic P, Rojas J, Birek C, Tenenbaum H, McCulloch CA (2001) Phenotypic comparison of periodontal ligament cells in vivo and in vitro. J Periodont Res 36(2): 71–79.
34. Murakami Y, Kojima T, Nagasawa T, Kobayashi H, Ishikawa I (2003) Novel isolation of alkaline phosphatase-positive subpopulation from periodontal ligament fibroblasts. J Periodontol 74(6): 780–786.
35. Shimabukuro Y, Ishikawa I, Takayama S, Yamada S, Takedachi M, et al. (2005) Fibroblast growth factor-2 regulates the synthesis of hyaluronan by human periodontal ligament cells. J Cell Physiol 203: 557–563.
36. Shimabukuro Y, Ishikawa T, Terashima Y, Iwayama T, Oohara H, et al. (2008) Basic fibroblast growth factor regulates expression of heparan sulfate in human periodontal ligament cells. Matrix Biol. In press.
37. Terashima Y, Shimabukuro Y, Terakura M, Ikezawa K, Hashikawa T, et al. (2008) Fibroblast growth factor-2 regulates expression of osteopontin in periodontal ligament cells. J Cell Physiol. In press.

Biochemical and Biophysical Research Communications 371 (2008) 191–196

Contents lists available at ScienceDirect

Biochemical and Biophysical Research Communications

journal homepage: www.elsevier.com/locate/ybbrc

PLAP-1/asporin inhibits activation of BMP receptor via its leucine-rich repeat motif

M. Tomoeda [a], S. Yamada [a], H. Shirai [b], Y. Ozawa [a], M. Yanagita [a], S. Murakami [a,*]

[a] Department of Periodontology, Division of Oral Biology and Disease Control, Osaka University Graduate School of Dentistry, 1-8 Yamadaoka, Suita, Osaka 565-0871, Japan
[b] Advanced Genomics, Molecular Medicine Laboratories, Astellas Pharma, 21 Miyukigaoka Tsukuba-city, Ibaraki 305-8585, Japan

ARTICLE INFO

Article history:
Received 24 March 2008
Available online 11 April 2008

Keywords:
PLAP-1
Asporin
SLRP
BMP-2
Smad
Leucine-rich repeat

ABSTRACT

We previously identified the novel gene, periodontal ligament-associated protein-1 (PLAP-1)/asporin and reported that PLAP-1/asporin inhibited bone morphogenetic protein-2 (BMP-2)-induced cytodifferentiation of periodontal ligament (PDL) cells probably by direct interaction with BMP-2. Here, we elucidated the detailed regulatory mechanism of this protein on BMP-2-induced cytodifferentiation of PDL cells. Recombinant PLAP-1/asporin inhibited BMP-2-induced cytodifferentiation of PDL cells and competitively prevented BMP-2 from binding to the BMP receptor-IB (BMPR-IB), resulting in inhibition of BMP-dependent activation of Smad proteins. The induction of mutation to the leucine-rich repeat (LRR) motif, especially LRR5, within PLAP-1/asporin rescued the inhibitory effect of PLAP-1/asporin on BMP-2. By contrast, a 26-amino acid peptide in the PLAP-1/asporin LRR5 sequence inhibited BMP-2 activity. Our findings indicate that PLAP-1/asporin inhibits BMP-2-induced differentiation of PDL cells resulting from inactivation of the BMP-2 signaling pathway and that LRR, especially LRR5 of PLAP-1/asporin, plays an important role in the PLAP-1/asporin–BMP-2 interaction.

The periodontal ligament (PDL) is a connective tissue that surrounds the roots of the tooth and attaches the roots to the alveolar bone to mechanically support teeth and to play nutritive and sensory roles [1]. Moreover, the PDL plays an important role as a reservoir of multipotential mesenchymal stem cells that can differentiate into mineralized tissue-forming cells such as osteoblasts and cementoblasts [2,3]. The PDL constitutively expresses mRNA of alkaline phosphatase (ALPase), type I collagen, periostin and Runx-2 [4], suggesting that the PDL possesses a strong potential for hard-tissue formation. However, the PDL tissue is never ossified *in vivo*. This indicates that inhibitory mechanisms for matrix mineralization constantly exist within the PDL.

In order to clarify the uniqueness of the PDL at the molecular level, we previously examined the gene expression profile and identified a novel gene, PLAP-1, which belongs to the small leucine-rich proteoglycan (SLRP) family class I [5]. Interestingly, we found that PLAP-1/asporin inhibited bone morphogenetic protein-2 (BMP-2)-induced cell differentiation probably by binding to BMP-2 directly [6].

In addition to the tissue-specific expression of BMP-2 and cell surface receptors, BMP-2 signaling is precisely regulated by certain classes of molecules. Some SLRP family proteins were reported to directly associate with transforming growth factor-beta (TGF-β) and BMP-4 and served as their antagonists/agonists appropriate to the circumstances [7–9].

The LRR motif is very widely distributed and has been found in more than 100 intracellular and extracellular proteins. This motif is well conserved from humans to insects, associates with metal ions, DNA, other proteins, and exerts a variety of functions [10]. Interestingly, previous reports showed that a high affinity binding site for decorin and TGF-β is located between LRR3-5 of the decorin core protein [11], and that decorin binds to collagen mainly through its LRR4-5 [12].

Based on these reports and structural characteristics, we elucidated the PLAP-1/asporin regulatory mechanism in detail on BMP-2-induced cytodifferentiation of PDL cells.

Materials and methods

Cell culture. We have established a mouse PDL cloned cell line, MPDL22, and maintained MPDL22 cells as previously described [6].

Generation of recombinant PLAP-1/asporin protein. Recombinant mouse PLAP-1/asporin protein was generated from *Escherichia coli*. Mouse PLAP-1/asporin cDNA expressing pET29b vector was gifted by Dr. Ikegawa, RIKEN (Tokyo, Japan). We expressed and extracted protein as previously described [13] and removed the LPS using the Detoxi-Gel Endotoxin Removing Gel (PIERCE, Rockford, IL, USA).

Alkaline phosphatase activity and cellular DNA content. ALPase activity was assessed according to the procedure of Bessay et al. and DNA content was measured using a modification of the method of Labarca and Pagien as previously described [6].

* Corresponding author. Fax: +81 6 6879 2934.
E-mail address: ipshiny@dent.osaka-u.ac.jp (S. Murakami).

0006-291X/$ - see front matter © 2008 Elsevier Inc. All rights reserved.
doi:10.1016/j.bbrc.2008.03.158

Real-time PCR analysis. The total RNA was extracted from MPDL22 cells using the RNA easy kit (Qiagen, Germantown, MD, USA) according to the manufacturer's protocol. About 0.4 μg of total RNA extract was reverse-transcribed with the High Capacity cDNA Reverse Transcriptase kit (Applied Biosystems, Foster-city, CA, USA) to generate the single-stranded cDNA. PCR reactions were carried out using the ABI 7300 Fast Real-Time PCR System (Applied Biosystems) with the Power SYBR® Green PCR Master Mix (Applied Biosystems) according to the manufacturer's protocol. All reactions were run in triplicate. The primer sequences are available upon request.

Competitive sequential immunoprecipitation assay for BMP-2 binding to the BMP receptor and Western blotting. We incubated 0.6 μg recombinant mouse BMPR-IB/ALK6/Fc chimera (R&D Systems, Inc., Minneapolis, MN, USA) with the Protein G sepharose (Amersham) in a rotator at 4 °C for 1 h. At the same time, we incubated 0.6 μg recombinant human BMP-2 and various doses of recombinant PLAP-1/asporin protein. Then we mixed them and incubated at 4 °C for 1 h. We collected the immunoprecipitated complex by centrifugation. This was then separated by SDS-PAGE and blotted onto PVDF membranes. As a primary antibody, we used rabbit anti-BMPR-IB antibody (H-44) (1:250; Santa Cruz Biotech, Santa Cruz, CA, USA) and streptavidin-conjugated goat anti-BMP-2/4 antibody (1:250; R&D Systems). As a secondary antibody, we used horseradish peroxidase-linked goat anti-rabbit IgG antibody (Cappel, Aurora, OH, USA) and horseradish peroxidase-linked anti-streptavidin antibody (Amersham). We detected immunoreactive proteins using the ECL plus kit (Amersham).

Western blotting for BMP-dependent Smad-1/5/8. MPDL22 cells treated with BMP-2 in the presence or absence of recombinant PLAP-1/asporin protein for 30 min were washed twice with ice-cold PBS, and lysed with the lysis buffer (50 mM Tris–HCl (pH 7.4), 1% NP-40, 0.25% sodium deoxycholate, 150 mM NaCl, 1 mM EDTA, 1 mM Na_3VO_4, 1 mM NaF, and a tablet of Complete Mini (Roche Diagnostic GmbH, Penzberg, Germany) per 10 ml). The protein concentrations of the cell lysates were measured using the BCA protein assay kit (PIERCE, Rockford, IL, USA) according to the manufacturer's instructions. As a primary antibody, we used mouse anti-Smad1 antibody (1:100; Santa Cruz Biotech) and rabbit anti-phospho-Smad1/5/8 antibody (1:500; Cell Signaling Technology, Beverly, MA, USA). As a secondary antibody, we used horseradish peroxidase-linked goat anti-mouse IgG antibody (Santa Cruz Biotech) and horseradish peroxidase-linked goat anti-rabbit IgG antibody (Cappel).

Building of the tertiary structural model of mouse PLAP-1/asporin. The tertiary structural model of mouse PLAP-1/asporin was built by the homology modeling technique. We chose the complex structure of bovine biglycan dimer (PDB Code 2FT3 [14]) as the template because the protein is the closest homologue of PLAP-1/asporin whose 3D-structure has been determined by X-ray crystallography. The alignment of PLAP-1/asporin and biglycan was carried out by the software Clustal W [15], and then a total of ten models were constructed by the software MOE (*Molecular Operating Environment*, version 2006.0801; Chemical Computing Group Inc., Montreal, Que., Canada.) We used the software JOY [16] to evaluate the models, and chose the best model for the inspection. The precise inspection was carried out by software MOE and Rasmol [17].

Generation of stable PLAP-1/asporin mutant overexpressing cell clones. PLAP-1/asporin/3XFLAG expression vector was prepared as previously described [6]. The plasmids harboring the cDNA for PLAP-1/asporin mutants, I (E194K), II (E194G), and III (R170E, R219E) were generated from the respective wild-type plasmid, PLAP-1/asporin/3XFLAG expression vector, by the Quick Change Site-Directed Mutagenesis kit (Stratagene, LA Jolla, CA, USA) in accordance with the manufacturer's protocol using the following primer pairs: forward, 5′-GCTTTACAT GTTTTGAAAATGAGTGCAAACCCTC-3′ and reverse, 5′-GAGGGTTTGCACTCATTTT CAAAACATG TAAAGC-3′ for E194K; forward, 5′-GCTTTACATGTTTTGGGAATGAGTG CAAACCCTC-3′ and reverse, 5′-GAGGGTTTGCACTCATTCCCAAAACATGTAAAGC-3′ for E194G; forward, 5′-CCCAAATCATTAGCAGAACTCGAAATTCATGATAATAAAG-3′ and reverse, 5′-CTTTATTATCATCATGAATTTCGAGTTCTGCTAATGATTTGGG-3′ for R170E; forward, 5′-GGTGACAGTATTCCATATCGAGATCGCTGAAGCAAAAC-3′ and reverse, 5′-GTTTTGCTTCAGCGATCTCGATATGGAATACTGTCACC-3′ for R219E. The sequence was verified by 310 Genetic Analyzer. We plated 5×10^4 of the MPDL22 cells per well in a 6-well plate (Corning Inc., Corning, NY, USA). After 24 h, we transfected the cells with the PLAP-1/asporin/3XFLAG expression vector using Effectene Transfection Reagent (Invitrogen, Carisbad, CA, USA) in accordance with the manufacturer's protocol. The cells were selected for neomycin resistance by adding 400 μg/ml G418 (Invitrogen).

Synthesis of the LRR5/PLAP-1/asporin peptide. We synthesized the 26-residue leucine-rich repeat 5 (LRR5) peptide of mouse PLAP-1/asporin core protein at Thermo Electron GmbH with amino acid sequence of ALHVLEMSANPLENNGIEP-GAFEGVT. We used a randomly scrambled sequence for the control peptide: TALEAPVEGPIGFLENNLEVHGSMNA. Amino-ethoxy-ethoxy-acetic acid was conjugated into the N-terminus for improving hydrophilicity.

Statistical analysis. All the experiments in this study were conducted at least three times. We show the representative results. Experimental values were given as means ± SD of triplicate assays. The statistical significance of the differences between two means was examined by the Mann–Whitney *U* test; *P* values less than 0.05 were considered to indicate a significant difference.

Results

PLAP-1/asporin inhibits BMP-2-induced cytodifferentiation

In our previous study, we showed that overexpression of PLAP-1/asporin inhibited BMP-2-induced cytodifferentiation [6]. To investigate the effect of PLAP-1/asporin on BMP-2-induced cytodifferentiation at the protein level, we treated MPDL22 with BMP-2 in the presence or absence of recombinant PLAP-1/asporin protein. N-terminal BAP control protein (SIGMA, St. Louis, MO, USA), which was a non-functional protein, was used as control. When the cells were treated with 0.5 μg and 1 μg recombinant PLAP-1/asporin protein, both BMP-2-induced ALPase activity and osterix mRNA expression were suppressed (Fig. 1A and B).

PLAP-1/asporin inhibits BMP-2 binding to BMPR-IB

We previously showed that PLAP-1/asporin binds to BMP-2 directly [6]. Thus, we speculated that the inhibitory effect of PLAP-1/asporin on BMP-2-induced cytodifferentiation of MPDL22 was caused by the inhibition of BMP-2 binding to the BMP receptor. To clarify this hypothesis, we performed the competitive sequential immunoprecipitation assay. In the presence of BAP control protein, BMP-2 was co-immunoprecipitated with BMPR-IB. However, the addition of recombinant PLAP-1/asporin reduced co-immunoprecipitated BMP-2 in a dose-dependent manner (Fig. 2A).

PLAP-1/asporin inhibits the phosphorylation of BMP-dependent Smad proteins

Since PLAP-1/asporin was revealed to prevent BMP-2 from binding to BMPR-IB, we further examined whether PLAP-1/asporin inhibited the BMP-dependent phosphorylation of Smads1/5/8. Western blotting analysis revealed that total Smad1/5/8 existed consistently and the phosphorylation of these Smads was initiated by BMP-2 stimulation, then after 30 min the phosphorylation reached the maximum level (data not shown). When we stimulated MPDL22 cells with BMP-2 in the presence of PLAP-1/asporin, the phosphorylation of Smad1/5/8 was inhibited (Fig. 2B).

Mutation to LRR5/PLAP-1/asporin rescues the PLAP-1/asporin inhibitory effects on BMP-2-induced cytodifferentiation

Since we revealed that PLAP-1/asporin directly binds to BMP-2, we further investigated the binding site of PLAP-1/asporin. A recent report revealed that decorin mutants, harboring an amino acid substitution of Glu-180 for Lys, showed differential interaction with types I and VI collagen [18]. In order to gain further insight into the molecular structure and function of PLAP-1/asporin, we first built a tertiary structural model of mouse PLAP-1/asporin (Fig. 3A and B). This model demonstrated that negatively charged Glu-194 of mouse PLAP-1/asporin corresponds to Glu-180 of human decorin, situated at the surface, and is sandwiched between positively charged Arg-170 (LRR4) and Arg-219 (LRR6). These ionic residues attracted our attention for their potential involvement in the PLAP-1/asporin–BMP-2 interaction.

Therefore, we induced mutation into these residues. We generated stable clones of MPDL22 cells expressing wild-type PLAP-1/asporin, mutant I (E194K), mutant II (E194G), and mutant III (R170E, R219E) (Fig. 3C). Although the cells expressing wild-type PLAP-1/asporin showed decreased levels of ALPase activity and osterix mRNA expression, the cells expressing mutant I (E194K) and mutant II (E194G) showed almost the same or rather high levels of ALPase activity and osterix mRNA expression compared with those of control cells. On the other hand, the cells expressing mu-

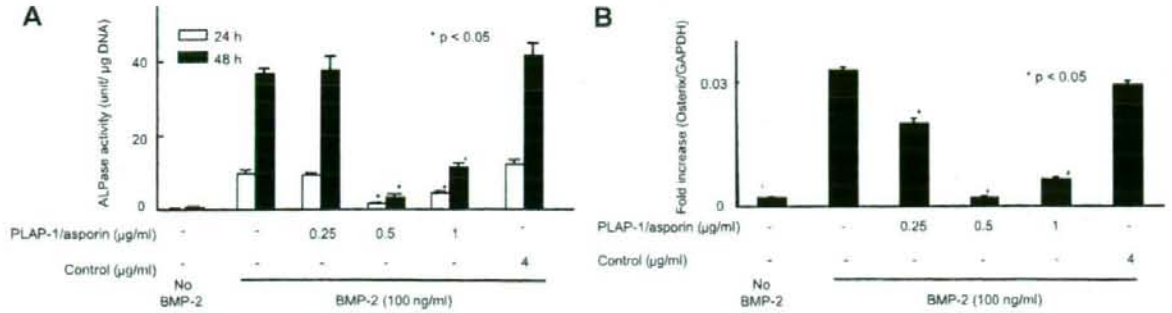

Fig. 1. PLAP-1/asporin inhibits BMP-2-induced cytodifferentiation. (A) ALPase activity in MPDL22 cells cultured for 24 h and 48 h with BMP-2 (100 ng/ml) in the presence or absence of PLAP-1/asporin recombinant protein at the indicated concentrations or N-terminal BAP control protein (4 μg/ml). (B) Real-time PCR analysis of osterix mRNA expression using total RNA isolated from the above-mentioned MPDL22 cells at 48 h treatment. Data represent means ± SEM in triplicate assays. $^*P < 0.05$ (Mann–Whitney U test) vs. N-terminal BAP control protein treatment.

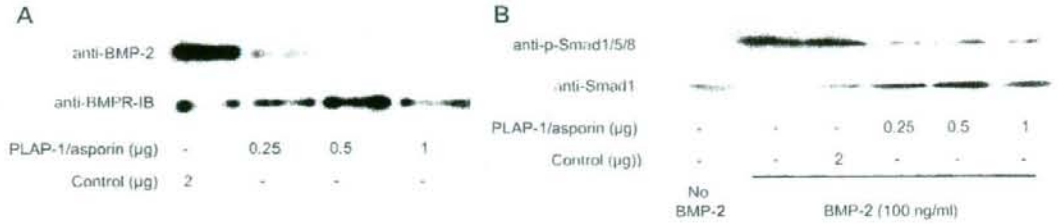

Fig. 2. PLAP-1/asporin inhibits BMP-2 binding to BMPR-IB and the sequential signal transduction. (A) PLAP-1/asporin inhibited BMP-2 binding to BMPR-IB. The competitive inhibition assay was performed. BMPR-IB was incubated with BMP-2 in the presence or absence of recombinant PLAP-1/asporin protein at the indicated concentrations or N-terminal BAP control protein (2 μg). In the presence of N-terminal BAP control protein, BMP-2 (upper panel) was co-immunoprecipitated with BMPR-IB (lower panel). The addition of PLAP-1/asporin reduced co-immunoprecipitated BMP-2 in a dose-dependent manner. (B) The effect of PLAP-1/asporin on the BMP-2-induced phosphorylation of Smad1/5/8 determined by Western blot analysis using anti-phospho-Smad1/5/8 antibody (upper panels). Whole cell extracts were lysed from MPDL22 cells after 30 min treatment with BMP-2 (100 ng/ml) in the presence or absence of recombinant PLAP-1/asporin protein at the indicated concentrations or N-terminal BAP control protein (2 μg). The lower panel shows the expression of Smad1 to demonstrate normalized loading of protein.

tant III (R170E, R219E) showed suppression of them, but the level of the suppression was approximately half compared to wild-type PLAP-1/asporin expressing cells (Fig. 3D and E).

LRR5/PLAP-1/asporin peptide inhibits BMP-2-induced cytodifferentiation

To further verify the contribution of LRR5 to the interaction between PLAP-1/asporin and BMP-2, we synthesized the 26-amino acid peptide within LRR5 of PLAP-1/asporin. The peptide which was randomly scrambled from the alignment of LRR5/PLAP-1/asporin was used as control (Fig. 4A). LRR5/PLAP-1/asporin at concentrations ranging from 0.1 μM to 10 μM showed inhibitory effects on BMP-2-induced ALPase activity and osterix mRNA expression (Fig. 4B and C). When we also stimulated MPDL22 cells with BMP-2 in the presence of LRR5/PLAP-1/asporin, the phosphorylation of Smad1/5/8 was inhibited (Fig. 4D) as was found with full length recombinant PLAP-1/asporin protein.

Discussion

In this paper, we revealed that PLAP-1/asporin acted as a negative regulator of BMP-2-induced cytodifferentiation of PDL cells *in vitro* by inhibiting BMP-Smads signal transduction via the center part of the LRR domain of PLAP-1/asporin.

Recombinant PLAP-1/asporin protein showed a BMP-2 inhibitory effect in PDL cells. This result was consistent with our previous finding that PLAP-1/asporin-overexpressing cells showed hyporesponsiveness to BMP-2. However the inhibitory effect of PLAP-1/asporin was not dose-dependent as was the case with the LRR5/PLAP-1/asporin peptide. This may be at least partially explained by the phenomenon that the expression of endogenous PLAP-1/asporin mRNA was significantly suppressed by adding of 1 μg/ml of PLAP-1/asporin (data not shown). Moreover, we previously reported that the expression of PLAP-1/asporin was induced by BMP-2 [19]. These facts indicate that PLAP-1/asporin and BMP-2 form a regulatory feedback loop. In Fig. 2B, Smad1 showed the tendency to decrease slightly as to correlate with its phosphorylation. However, this correlation did not necessarily occur and was not reproducible as seen in Fig. 4D. With the present date, we consider that the phosphorylation of Smad1 may not correlate with its degradation.

Having clarified that PLAP-1/asporin directly binds to BMP-2, we then tried to identify the site(s) which would be involved in the molecular interaction. It has been proposed that decorin binds to TGF-β and collagen through LRR3-5 [11] or LRR4-5 [12]. In addition, peptides derived from human decorin LRR5 have been reported to inhibit angiogenesis [20]. We found in this study that LRR5/PLAP-1/asporin exerted biological activity in inhibiting BMP-2-induced cytodifferentiation. LRR5/decorin was reported to have the same secondary structure as LRR5 of mature decorin. As PLAP-1/asporin shows high conservation of residues compared to decorin, LRR5/PLAP-1/asporin may also have structural effects.

We built a 3D-structural model of mouse PLAP-1/asporin and found ionic residues at the center of the concave surface which might be involved in the PLAP-1/asporin–BMP-2 interaction.

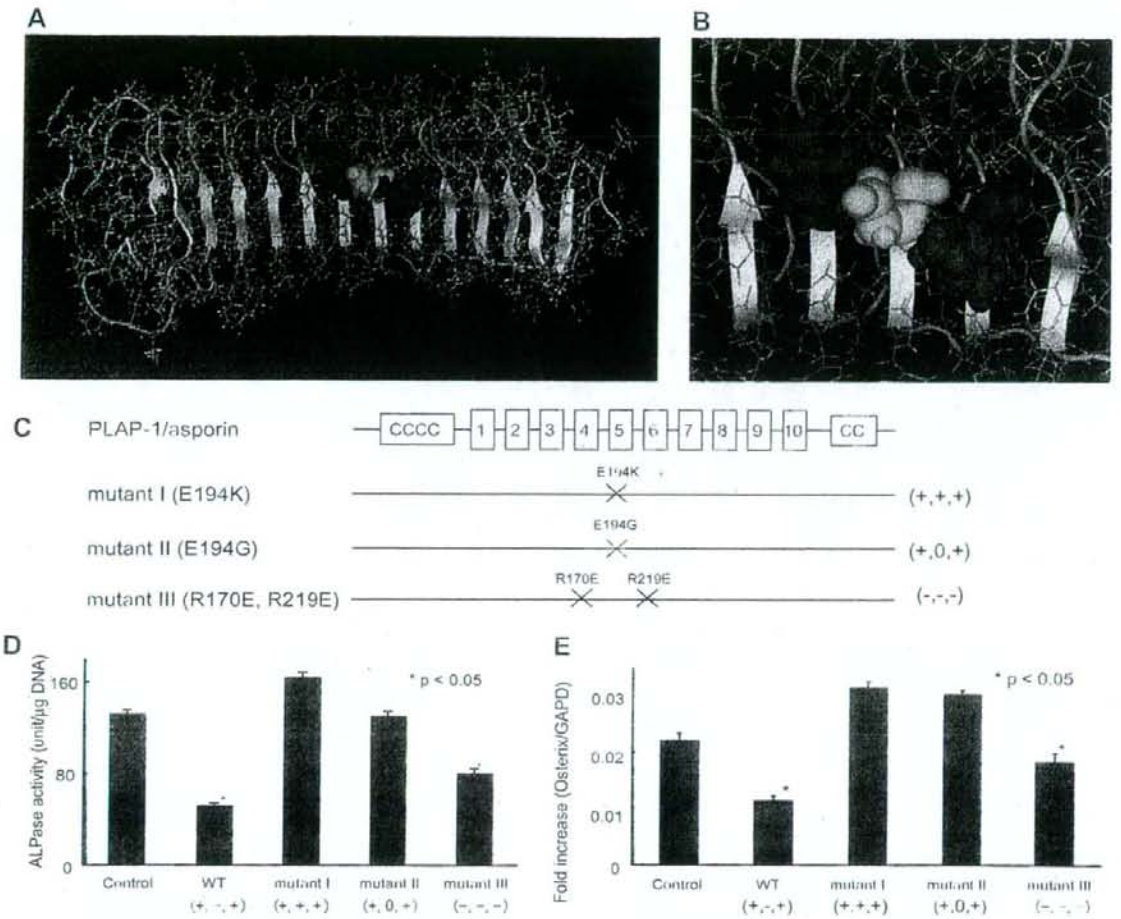

Fig. 3. Mutation to LRR5/PLAP-1/asporin rescues the inhibitory effects of PLAP-1/asporin on BMP-2-induced cytodifferentiation. (A) Schematic representation of the model structure of mouse PLAP-1/asporin viewed from the concave surface. The overall feature is a typical long leucine-rich repeat fold, and the molecular surface is occupied with many aromatic and charged residues. In general, protein/protein interactions prefer strong hydrophobic interaction by using aromatic residues. The existence of charged residues would probably make the monomer stable as well as the dimer conformation. (B) Close-up view of the potential binding site. Glu-194 is shown in green space-fill in the model and Arg-170 (right side) and Arg-219 (left side) are shown in purple space-fill. The other residues are shown in line and their carbon, nitrogen, hydrogen and oxygen atoms are colored in gray, blue, white and red, respectively. The secondary structure is represented with ribbon; the β-sheet is drawn in yellow, turn in blue, loop in cyan and helix in red. (C) Schematic structure of PLAP-1/asporin. PLAP-1/asporin contains 10 LRRs in the core protein. We introduced the single nucleotide mutation, for mutant I (Glu-194 to Lys), mutant II (Glu-194 to Gly), and mutant III (Arg-170 to Glu, Arg-219 to Glu). Letters on the right side indicate the charge of residues 170, 194, and 219 after the induction of the mutation. (D) ALPase activity in MPDL22 cells stably expressing wild-type or mutant PLAP-1/asporin cultured for 48 h with BMP-2 (100 ng/ml). MPDL22 stably transfected with expression vector was the control. Letters under the vector name indicate the charge of residues 170, 194, and 219. (E) Real-time PCR analysis of osterix mRNA expression using total RNA isolated from the above-mentioned MPDL22 transfectants. Letters under the vector name indicate the charge of residues 170, 194, and 219. Data represent means ± SEM in triplicate assays. $^{*}P < 0.05$ (Mann–Whitney *U* test) vs. control. (For interpretation of color mentioned in this figure the reader is referred to the web version of the article.)

Therefore, we generated mutants of mouse PLAP-1/asporin. The cells expressing mutant I (E194K) and mutant II (E194G) showed almost equivalent ALPase activity and osterix mRNA expression to control but the cells expressing mutant III (R170E, R219E) showed half the inhibition for BMP-2 stimulation compared to wild-type PLAP-1/asporin. To introduce the mutation Glu-194 for Lys (mutant I), positively charged residues were gathered at the center of the concave surface, whereas to introduce the mutation Arg-170 and Arg-219 for Glu (mutant III), negatively charged residues were gathered. Although each of them exhibited ionic instability, mutant I showed complete rescue but mutant III showed half rescue. This fact raised the possibility that Glu-194 (LRR5) of PLAP-1/asporin plays a critical role in the interaction with BMP-2 and that Arg-170 and Arg-219 would be supportive. It was reported that biologically active decorin was a monovalent ligand for various extracellular matrix proteins, growth factors, and cell surface receptors [21]. However the other report challenged this view. The concave surface of decorin was involved in a high-affinity dimer interaction, and, therefore, was unlikely to be available for ligand binding [22]. The sites where we introduced the mutation were considered to be involved in direct contact at the dimer interface in terms of this report. There is the possibility that Glu-194 and surrounding charged residues are not the exact residues to bind to BMP-2 but the residues involved in the dimer-to-monomer transition of PLAP-1/asporin, which leads to the association of PLAP-1/asporin with BMP-2. Although there exists such contradic-

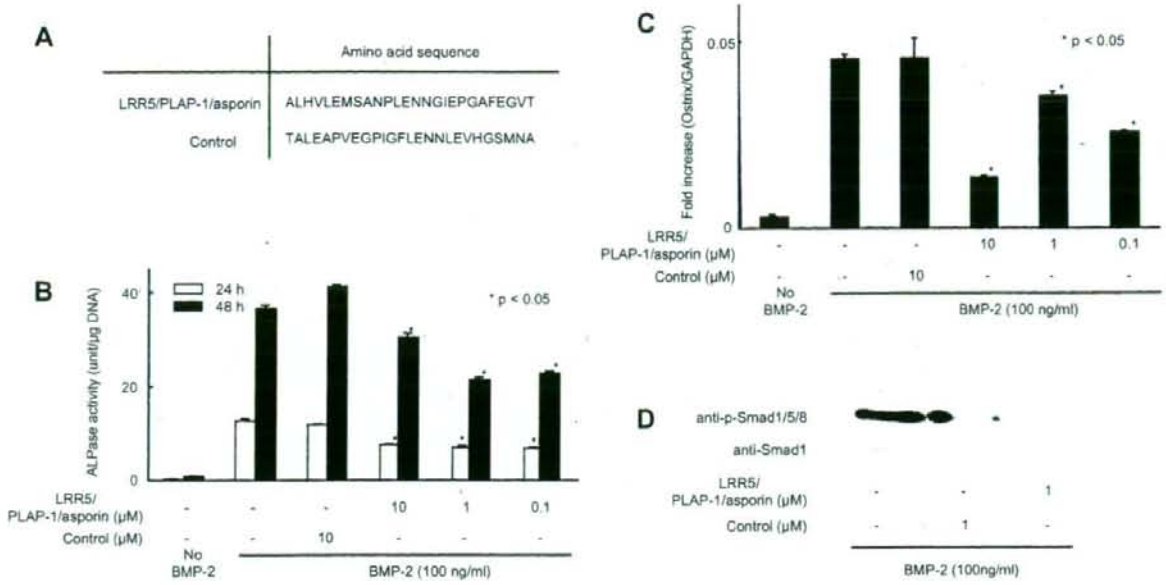

Fig. 4. LRR5/PLAP-1/asporin peptide inhibits the BMP-2-induced cytodifferentiation. (A) The amino acid sequences of LRR5/PLAP-1/asporin and control peptides. (B) ALPase activity in MPDL22 cells cultured for 24 h and 48 h with BMP-2 (100 ng/ml) in the presence or absence of LRR5/PLAP-1/asporin at indicated concentrations or control (10 μM). (C) Real-time PCR analysis of osterix mRNA expression using total RNA isolated from the above-mentioned MPDL22 cells of 48 h treatment. Data represent means ± SEM in triplicate assays. $^{*}P < 0.05$ (Mann–Whitney *U* test) vs. control peptide treatment. (D) The effect of LRR5/PLAP-1/asporin on the BMP-2-induced phosphorylation of Smad1/5/8 determined by Western blot analysis using anti-phospho-Smad1/5/8 antibody (upper panels). Whole cell extracts were lysed from MPDL22 cells after 30 min treatment with BMP-2 (100 ng/ml) in the presence or absence of LRR5/PLAP-1/asporin (1 μM) or control (1 μM). The lower panel shows the expression of Smad1 to demonstrate normalized loading of protein.

tion at the present, our results using the LRR5/PLAP-1/asporin peptide strongly suggests the direct interaction via LRR5 between PLAP-1/asporin and BMP-2. The detailed role of the central LRR and the residues within it upon the PLAP-1/asporin–BMP-2 interaction needs to be elucidated using PLAP-1/asporin protein in future studies.

This work is first to report the structure–function relationship between PLAP-1/asporin and BMP-2. PLAP-1/asporin can inhibit BMP-2-induced cytodifferentiation via the center part of LRR, especially LRR5, so that the PDL would not be mineralized but act as the connective tissue showing high osteoblastic potential *in vivo*.

Acknowledgments

This work was supported by Grants-in-Aid for Scientific Research from the Japan Society for the Promotion of Science (Nos. 17390560, 17390561, 19771611), and the 21st Century COE entitled "Osaka University Graduate School of Dentistry supported by the Ministry of Education, Culture, Sports, Science and Technology. It was also supported by a grant from the Smoking Research Foundation.

References

[1] W. Beertsen, C.A. McCulloch, J. Sodek, The periodontal ligament: a unique, multifunctional connective tissue, Periodontol 2000 13 (1997) 20–40.
[2] P. Lekic, C.A. McCulloch, Periodontal ligament cell population: the central role of fibroblasts in creating a unique tissue, Anat. Rec. 245 (1996) 327–341.
[3] B.M. Seo, M. Miura, S. Gronthos, P.M. Bartold, S. Batouli, J. Brahim, M. Young, P.G. Robey, C.Y. Wang, S. Shi, Investigation of multipotent postnatal stem cells from human periodontal ligament, Lancet 364 (2004) 149–155.
[4] Y. Saito, T. Yoshizawa, F. Takizawa, M. Ikegame, O. Ishibashi, K. Okuda, K. Hara, K. Ishibashi, M. Obinata, H. Kawashima, A cell line with characteristics of the periodontal ligament fibroblasts is negatively regulated for mineralization and Runx2/Cbfa1/Osf2 activity, part of which can be overcome by bone morphogenetic protein-2, J. Cell Sci. 115 (2002) 4191–4200.
[5] S. Yamada, S. Murakami, R. Matoba, Y. Ozawa, T. Yokokoji, Y. Nakahira, K. Ikezawa, S. Takayama, K. Matsubara, H. Okada, Expression profile of active genes in human periodontal ligament and isolation of PLAP-1, a novel SLRP family gene, Gene 275 (2001) 279–286.
[6] S. Yamada, M. Tomoeda, Y. Ozawa, S. Yoneda, Y. Terashima, K. Ikezawa, S. Ikegawa, M. Saito, S. Toyosawa, S. Murakami, PLAP-1/asporin, a novel negative regulator of periodontal ligament mineralization, J. Biol. Chem. 282 (2007) 23070–23080.
[7] Y. Yamaguchi, D.M. Mann, E. Ruoslahti, Negative regulation of transforming growth factor-beta by the proteoglycan decorin, Nature 346 (1990) 281–284.
[8] A. Hildebrand, M. Romaris, L.M. Rasmussen, D. Heinegard, D.R. Twardzik, W.A. Border, E. Ruoslahti, Interaction of the small interstitial proteoglycans biglycan, decorin and fibromodulin with transforming growth factor beta, Biochem. J. 302 (Pt 2) (1994) 527–534.
[9] X.D. Chen, L.W. Fisher, P.G. Robey, M.F. Young, The small leucine-rich proteoglycan biglycan modulates BMP-4-induced osteoblast differentiation, FASEB J. 18 (2004) 948–958.
[10] S.G. Buchanan, N.J. Gay, Structural and functional diversity in the leucine-rich repeat family of proteins, Prog. Biophys. Mol. Biol. 65 (1996) 1–44.
[11] E. Schonherr, M. Broszat, E. Brandan, P. Bruckner, H. Kresse, Decorin core protein fragment Leu155-Val260 interacts with TGF-beta but does not compete for decorin binding to type I collagen, Arch. Biochem. Biophys. 355 (1998) 241–248.
[12] L. Svensson, D. Heinegard, A. Oldberg, Decorin-binding sites for collagen type I are mainly located in leucine-rich repeats 4-5, J. Biol. Chem. 270 (1995) 20712–20716.
[13] H. Kizawa, I. Kou, A. Iida, A. Sudo, Y. Miyamoto, A. Fukuda, A. Mabuchi, A. Kotani, A. Kawakami, S. Yamamoto, A. Uchida, K. Nakamura, K. Notoya, Y. Nakamura, S. Ikegawa, An aspartic acid repeat polymorphism in asporin inhibits chondrogenesis and increases susceptibility to osteoarthritis, Nat. Genet. 37 (2005) 138–144.
[14] P.G. Scott, C.M. Dodd, E.M. Bergmann, J.K. Sheehan, P.N. Bishop, Crystal structure of the biglycan dimer and evidence that dimerization is essential for folding and stability of class I small leucine-rich repeat proteoglycans, J. Biol. Chem. 281 (2006) 13324–13332.
[15] J.D. Thompson, D.G. Higgins, T.J. Gibson, CLUSTAL W: improving the sensitivity of progressive multiple sequence alignment through sequence weighting, position-specific gap penalties and weight matrix choice, Nucleic Acids Res. 22 (1994) 4673–4680.
[16] K. Mizuguchi, C.M. Deane, T.L. Blundell, M.S. Johnson, J.P. Overington, JOY: protein sequence-structure representation and analysis, Bioinformatics 14 (1998) 617–623.

[17] R.A. Sayle, E.J. Milner-White, RASMOL: biomolecular graphics for all, Trends Biochem. Sci. 20 (1995) 374.
[18] G. Nareyeck, D.G. Seidler, D. Troyer, J. Rauterberg, H. Kresse, E. Schonherr, Differential interactions of decorin and decorin mutants with type I and type VI collagens, Eur. J. Biochem. 271 (2004) 3389–3398.
[19] S. Yamada, Y. Ozawa, M. Tomoeda, R. Matoba, K. Matsubara, S. Murakami, Regulation of PLAP-1 expression in periodontal ligament cells, J. Dent. Res. 85 (2006) 447–451.
[20] K.N. Sulochana, H. Fan, S. Jois, V. Subramanian, F. Sun, R.M. Kini, R. Ge, Peptides derived from human decorin leucine-rich repeat 5 inhibit angiogenesis, J. Biol. Chem. 280 (2005) 27935–27948.
[21] S. Goldoni, R.T. Owens, D.J. McQuillan, Z. Shriver, R. Sasisekharan, D.E. Birk, S. Campbell, R.V. Iozzo, Biologically active decorin is a monomer in solution, J. Biol. Chem. 279 (2004) 6606–6612.
[22] P.G. Scott, P.A. McEwan, C.M. Dodd, E.M. Bergmann, P.N. Bishop, J. Bella, Crystal structure of the dimeric protein core of decorin, the archetypal small leucine-rich repeat proteoglycan, Proc Natl Acad Sci U S A 101 (2004) 15633–15638.

Nicotine Inhibits Mineralization of Human Dental Pulp Cells

Manabu Yanagita, DDS, PhD, Yoichiro Kashiwagi, DDS, Ryohei Kobayashi, DDS, PhD, Miki Tomoeda, DDS, PhD, Yoshio Shimabukuro, DDS, PhD, and Shinya Murakami, DDS, PhD

Abstract

Nicotine is a major component of tobacco smoke, and signals via nicotinic acetylcholine receptors (nAChR). However, little is known about the effects of nicotine on human dental pulp cells (HDPCs). In this study, we assessed the effects of nicotine on mineralization in HDPCs. We confirmed messenger RNA expression of nAChR subunits and examined the effects of nicotine on expression of extracellular matrices (ECMs), alkaline phosphatase (ALP) activity, and mineralized nodule formation by HDPCs. Gene expression of nAChR subunits $\alpha1$, $\alpha2$, $\alpha4$, $\alpha5$, $\alpha6$, $\alpha7$, $\beta1$, $\beta2$, and $\beta4$ was detected in HDPCs. Interestingly, the messenger RNA expression of dentin matrix acidic phosphoprotein-1, bone sialoprotein, and ALP activity were significantly reduced in nicotine-treated HDPC. In addition, mineralized nodule formation, which was examined by alizarin red staining, was also inhibited in HDPCs by the same treatment. These results indicate that nicotine suppresses the cytodifferentiation and mineralization of HDPCs, possibly via nAChR. *(J Endod 2008;34:1061–1065)*

Key Words

Dental pulp cells, mineralization, nicotine

From the Department of Periodontology, Division of Oral Biology and Disease Control, Osaka University Graduate School of Dentistry, Osaka, Japan.

Supported in part by the 21st Century COE entitled "Origination of Frontier BioDentistry" at Osaka University Graduate School of Dentistry; the Ministry of Education, Culture, Sports, Science and Technology; and a grant from the Smoking Research Foundation.

Address requests for reprints to Dr Shinya Murakami, Department of Periodontology, Division of Oral Biology and Disease Control, Osaka University Graduate School of Dentistry, 1-8 Yamadaoka, Suita, Osaka 565-0871, Japan. E-mail address: ipshinya@dent.osaka-u.ac.jp.

0099-2399/$0 - see front matter

doi:10.1016/j.joen.2008.06.005

Tobacco smoking is associated with the development of numerous diseases such as cancers, vascular diseases, chronic obstructive pulmonary diseases, and periodontal diseases (1–3). Nicotine is one of the main components of tobacco smoke and a selective agonist of nicotinic acetylcholine receptors (nAChRs). Human nAChRs are pentamers that are ligand-gated ion channels consisting of α-subunits ($\alpha1\sim\alpha7$, $\alpha9$, and $\alpha10$), β-subunits ($\beta1\sim\beta4$), and ε, γ, and δ subunits (4). So far, two types of pentamer have been revealed: one is muscle nAChR, and the other is neuronal nAChR. Muscle nAChRs were first identified at the neuromuscular junction and contain $\alpha1/\beta1/\varepsilon/\delta$ subunits. On the other hand, the expression of neuronal nAChR was discovered in the central nervous system, and these nAChRs contain $\alpha2\sim\alpha7$, $\alpha9$, $\alpha10$, and $\beta2\sim\beta4$ subunits. Interestingly, it has been recently been reported that these receptors are also expressed on epithelial cells (5), fibroblasts (6), lymphocytes (7), and alveolar macrophages (8).

Tooth injury and dental caries induce reactionary or reparative dentinogenesis. It has been well known that dental pulp contains cells capable of regenerating dentin/pulp complex (9). In fact, previous reports showed that cultured dental pulp cells form calcified nodules in vitro (10). On the other hand, it was recently shown that odontoblasts generated in vitro from human dental pulp explants responded to cariogenic bacteria and decreased the function of dentin matrix synthesis and mineralization (11).

Nicotine has been shown to inhibit bone growth, to depress osteoblast activity (12), and to impair bone repair (13). However, nicotine has also been reported to stimulate alkaline phosphatase activity in rat osteoblastic cells (14) and induce osteoblastic cell proliferation (15). These reports suggest that nicotine can modulate the functions of osteoblastic lineage cells.

Because little is known about the effects of nicotine on human dental pulp cells (HDPCs), we investigated the expression of nAChR and the effects of the ligand, nicotine, on cytodifferentiation and mineralization in HDPCs.

Materials and Methods

Culture of HDPCs

HDPCs were isolated from healthy dental pulp of first premolar teeth of individuals undergoing tooth extraction for orthodontic treatment, as described previously in detail (16). All the patients gave informed consent before collection of samples, and the protocols were approved by the Institutional Review Board of Osaka University Graduate School of Dentistry. In this study, we established three cell lines from different volunteers, and all cell lines were used in each experiment. After the cells reached confluence, we replaced the culture medium (α-Eagle's minimum essential medium [MEM] supplemented with 10% fetal calf serum [FCS]) with the mineralization medium (α-MEM supplemented with 10% FCS, 10 mmol/L β-glycerophosphate, and 50 μg/mL ascorbic acid). We replaced the mineralization medium every 3 days with or without nicotine (1 mmol/L or 10 nmol/L), which was prepared in PBS and neutralized to pH 7.2.

Detection of nAChRs in HDPCs by Real-time Polymerase Chain Reaction

HDPCs were seeded at a density of 10^5 cells/dish in a 60-mm dish and grown to confluency with α-MEM supplemented with 10% FCS. After culture of HDPCs with or without nicotine, total RNA was extracted from each cell by RNAbee (TEL-TEST, Friedswood, TX) according to the manufacturer's instructions. Complementary DNA synthe-

TABLE 1. Real-Time PCR Primers for nAChR Subunits Used in This Study

Gene		Primer	Reference
alpha1	Forward	5′-CCA GAC CTG AGC AAC TTC ATG G-3′	10
	Reverse	5′-AAT GAG TCG ACC TGC AAA CAC G-3′	
alpha2	Forward	5′-TGA CCC ACA TGA CCA AGG CCC A-3′	22
	Reverse	5′-TGG TGA ACA GCA GGT ACT CGC C-3′	
alpha3	Forward	5′-CCG AGG CCC CTC TAC GGT-3′	23
	Reverse	5′-CAC ACA GCT TAG TGC TTA-3′	
alpha4	Forward	5′-CAC GTT TGC CAA ATT TTC CT-3′	24
	Reverse	5′-CCG AGT CCT GCA GGT AGA AG-3′	
alpha5	Forward	5′-CCA TCA TCT TCA AAA GTC ATA-3′	23
	Reverse	5′-CCC ATT TAT AAA TAA CAG GAA C-3′	
alpha6	Forward	5′-GCT GTG CAA CTG AGG AGA GGC T-3′	22
	Reverse	5′-AAG ACG GTG AGC GAC AGC AGC-3′	
alpha7	Forward	5′-CCC AAG TGG ACC AGA GTC AT-3′	10
	Reverse	5′-GAT GTA CAG CAG GTT CCC GT-3′	
alpha9	Forward	5′-CGA GAT CAG TAC GAT GGC CTA G-3′	10
	Reverse	5′-TCT GTG ACT AAT CCG CTC TTG C-3′	
alpha10	Forward	5′-TCT CAA GCT GTT CCG TGA CC-3′	25
	Reverse	5′-AAG GCT GCT ACA TCC ACG C-3′	
beta1	Forward	5′-GTG TCA GGG TCA GGG TTG GT-3′	26
	Reverse	5′-TGC GGC GGA TGA TGA GGT AG-3′	
beta2	Forward	5′-GGC ATG TAC GAG GTG TCC TT-3′	24
	Reverse	5′-CAC CTC ACT CTT CAG CAC CA-3′	
beta3	Forward	5′-AAG GGG AAC AGA AGG GAC GG-3′	22
	Reverse	5′-GAA GCA GTA CGT CGC GGA CG-3′	
beta4	Forward	5′-GTT CAT GTT TGT GTG CGT CC-3′	24
	Reverse	5′-AAC CCA GAA AGA AGC AGC AA-3′	
HPRT	Forward	5′-CGA GAT GTG ATG AAG GAG ATG GG-3′	20
	Reverse	5′-GCC TGA CCA AGG AAA GCA AAG TC-3′	

sis and amplification via polymerase chain reaction (PCR) were performed, as described previously (17). The primers used for PCR are listed in Table 1 (8, 16, 18–21). After denaturation at 95°C for 5 minutes, each cycle consisted of 95°C for 1 minute, 55°C for 1 minute, and 72°C for 1 minute. Amplified products were analyzed by electrophoresis at 100 V for 30 minutes on 1.5% tris-acetate - EDTA agarose gels containing 0.5 μg/mL ethidium bromide. Human brain and muscle RNA samples (TAKARA-Bio Inc, Otsu, Japan) were used as a positive control for nAChR subunits (muscle for α1 and β1 and brain for α2-7, α9-10, and β2-4).

Quantitative Real-time PCR for Extracellular Matrices

Real-time PCR was performed with an ABI 7700 system (Applied Biosystems, Tokyo, Japan). Reactions were performed according to the manufacturer's protocol. The primers used for real-time PCR were as follows: hypoxanthine phosphoribosyl transferase (HPRT), (sense) 5′-GGC AGT ATA ATC CAA AGA TGG TCA A-3′ and (antisense) 5′-GTC AAG GGC ATA TCC TAC AAC AAA C-3′; collagen type I, (sense) 5′-CTG CTG GAC GTC CTG GTG-3′ and (antisense) 5′-ACG CTG TCC AGC AAT ACC TTG-3′; bone sialoprotein (BSP), (sense) 5′-CTG GCA GGG TAC AGG GTT AG-3′ and (antisense) and 5′-ATC GGT GCC GTT TAT GCC TTG-3′; dentin matrix acidic phosphoprotein (DMP)-1, (sense) 5′-AGA TCA GCA TCC TGC TCA TGT TC-3′ and (antisense) 5′-TGG TGC CTG AGC CAA ATG AC-3′; and dentin sialophosphoprotein, (sense) 5′-TGG AGA CAA GAC CTC CAA GAG TGA-3′ and (antisense) 5′-TGC TGG GAC CCT TGA TTT CTA TTC-3′.

Alkaline Phosphatase Activity and Mineralization Assay

Alkaline phosphatase activity (ALP) activity was assessed according to the procedure described previously (22). In brief, after washing twice with PBS, cells were homogenized in 1 mL 0.9% NaCl and 0.2% Triton-X-100 (Wako, Osaka, Japan) at 4°C in a glass homogenizer and then centrifuged for 15 minutes at 12,000g. ALP activity in the supernatant was measured by using p-nitrophenyl phosphate (pNP) as a substrate. Subsequently, the supernatant was mixed with 0.5 mol/L tris-HCl buffer (pH 9.0) containing 0.5 mmol/L pNP and 0.5 mmol/L MgCl2. Next, the samples were incubated at 37°C for 30 minutes, and the reaction was stopped by addition of 0.25 mL 1 mol/L NaOH. Using a spectrometer, hydrolysis of pNP was monitored as a change in A410nm; p-nitrophenol was used as a standard. One unit of activity was defined as the enzyme activity hydrolyzing 1 nmol pNP in 30 minutes. Histochemistry for staining calcified nodules was performed by using the alizarin red staining method (23). Cell layers were washed twice with PBS and then fixed in dehydrated ethanol. After fixation, the cell layers were stained with 1% alizarin red S in 0.1% NH_4OH (pH 6.3–6.5) for 5 minutes. The dishes were washed with H_2O and then observed microscopically, digitized, and analyzed by using the WinRoof software program (Mitani Corporation, Fukui, Japan).

Statistical Analysis

Statistical analysis of the results was performed by one-way analysis of variance. Differences were considered statistically significant when p values were less than 0.05.

Results

Neuronal and Muscle-type nAChR Are Expressed on HDPCs

We examined the expression of nAChR subunit messenger RNA on HDPCs using real-time PCR. As shown in Figure 1A, we found that all HDPCs expressed messenger RNA for muscle-type nAChR subunits (α1and β1) and neuronal-type nAChR subunits (α2, α4, α5, α6, α7, β2, and β4). However nAChR subunits α3, α9, α10, and β3 were not detected in HPDC.

Nicotine Reduces Messenger RNA Expression of Extracellular Matrices in HDPCs

We then examined the effects of nicotine (10^{-3} mol/L) on gene expression of the extracellular matrices (ECMs) (Fig. 1*B*). HDPCs that

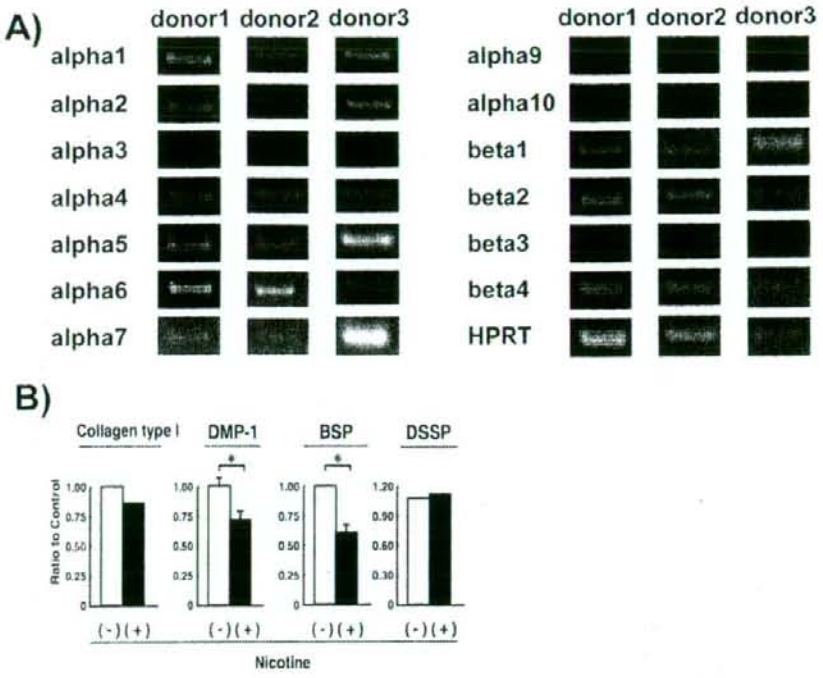

Figure 1. (*A*) The expression of nAChR messenger RNA in HDPCs. Results of three different donors are shown. The number of PCR cycles is 30 and 24 for nAChRs and HPRT, respectively. (*B*) The analysis of messenger RNA expression in ECM by real-time PCR. RNA samples were obtained from HDPC 2 days after nicotine treatment (10^{-5} mol/L). The relative expression of each ECM was standardized against the amount in HPRT and the expression of ECM in HDPC without nicotine has been taken as 1.0. Values are means ± standard deviation of three determinations. *$p < 0.05$ compared with nontreated.

were treated with nicotine showed significantly decreased messenger RNA expression of DMP-1 and BSP. However, nicotine did not affect the gene expression of collagen type I and dentin sialophosphoprotein.

Nicotine Inhibits Mineralized Nodule Formation in HDPCs

We cultured HDPCs with or without nicotine in mineralization medium and then examined ALP activity and mineralized nodule formation by the HDPCs. Nicotine significantly inhibited ALP activity of HDPCs compared with that of HDPCs cultured in the absence of nicotine (Fig. 2*A*). Next, we investigated mineralized nodule formation by HDPCs on day 24. As shown in Figure 2*B*, nicotine reduced alizarin red staining intensity. Interestingly, even a low concentration of nicotine (10^{-8} mol/L) decreased mineralized nodule formation by the HDPCs.

Discussion

To the best of our knowledge, we provide evidence for the first time that HDPCs express neuronal nAChR subunits α2, α4, α5, α6, α7, β2, and β4 and muscle nAChR subunits α1 and β1 as assessed by real-time PCR. Among cells that have the ability to be calcified or mineralized, there has been only one previous report that the α4 nAChR was expressed in human primary osteoblasts (24). Previous studies reported that human gingival fibroblasts responded to nicotine. However, the expression of nAChR was not investigated (25). We also examined nAChR expression in human gingival fibroblasts and observed the same pattern of expression of nAChR as was found in HDPCs (unpublished data). As well as in neural cells, nAChR have been reported to be expressed on bronchial epithelial cells (HBECs). The stimulation of HBECs with nicotine induced calcium influx, which was inhibited by nAChR antagonists (26). However, not all subunits of nAChR expressed at messenger RNA levels were detected at protein levels in HBECs (26). Although the present study suggests that HDPCs express functional nAChR, it will be necessary to examine the protein level of nAChR expression in HDPCs.

Nicotine has been reported to have several positive and negative effects on host defense and reparative responses (3). We examined the expression of some ECMs, which are closely associated with mineralization, and revealed by real-time PCR that nicotine reduced the messenger RNA expression of DMP-1 and BSP (Fig. 1*B*). In addition, nicotine suppressed the induction of ALP activity (Fig. 2*A*) and reduced calcified nodule formation (Fig. 2*B*). These findings suggest that nicotine decreases the expression of ECM involved in mineralization and negatively regulates the mineralization of HDPCs probably via nAChR. Both DMP-1 and BSP are small integrin-binding ligand N-linked glycoproteins and are involved in the regulation of mineralization (27). So far, there are only a few reports describing the effect of nicotine on the expression of ECMs related to mineralization. Those studies showed that nicotine upregulated osteopontin expression in human primary osteoblastic cells (24) and that nicotine induced BSP and collagen type I but downregulated osteopontin in osteosarcoma cell lines (28). In addition, the present study suggests that nicotine plays a role as a negative regulator in the mineralization of HDPCs by reducing ECM expression. Thus, the effects of nicotine on ECM are still controversial and may be dependent on each cell type.

It is well known that smoking is a risk factor for the progression of periodontal diseases (3) and that nicotine alters the cellular functions of periodontal ligament cells and gingival fibroblasts (29). Nicotine concentration is known to reach mM levels in the saliva of deep inhalers of smoke (30), and periodontal tissues are considered to be exposed to

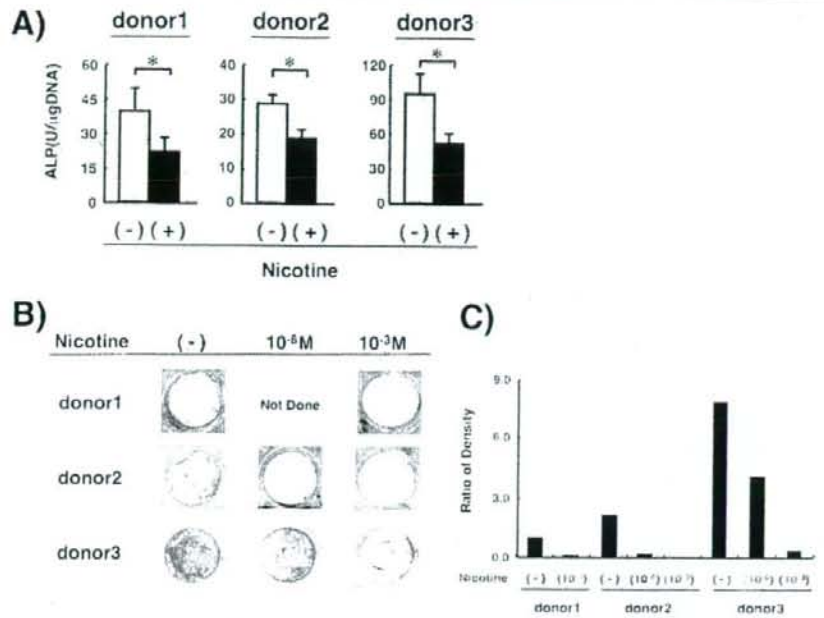

Figure 2. (*A*) The effects of nicotine on ALP activity in HDPCs. As described in the Materials and Methods section, HDPCs were cultured in 24-well plates in the presence or absence of nicotine for 21 days, and ALP activities were measured. Values are means ± standard deviation of three determinations. *$p < 0.05$ compared with nontreated. (*B*) The effects of nicotine (10^{-8} mol/L or 10^{-3} mol/L) on mineralization in HDPCs. Alizarin red staining was performed after 24 days of culture in mineralization medium. Results of one representative experiment out of three identical experiments are shown, and (*C*) the relative expression of value of alizarin stain of each data shown in Figure 2*B* was quantitated and normalized to alizarin stain without nicotine of donor 1.

a similar concentration of nicotine. In fact, it has been reported that smokers showed impaired periodontal tissue regeneration compared with nonsmokers (31). The other report suggested smoking may be a risk factor in the outcome of endodontic restorations and implant treatment (32). On the other hand, there is little information about the correlation between smoking and the regeneration of the dentin/pulp complex. Because the nicotine concentration in smokers' sera was 25 to 444 nmol/L (33), nicotine concentration in the dental pulp tissues of smokers is expected to be at 10 to 1,000 nmol/L levels. Figure 2*B* and *C* showed that even 10 nmol/L nicotine reduced calcified nodule formation. This suggests the possibility that a low concentration of nicotine circulating in the blood stream can suppress calcified nodule formation and that nicotine or cigarette smoke constituents can reduce reactionary or reparative dentinogenesis.

Nicotine is known to activate several mitogen-activated protein kinase signaling pathways in a variety of cell types. Among mitogen-activated protein kinases, it has been reported that nicotine stimulation rapidly increases extracellular signal-regulated kinase (ERK) 1/2 activation (34). ERK1/2 is involved in cellular growth and differentiation in response to various cytokines and growth factors. Although previous reports suggested that nicotine has cytotoxicity (29), we did not observe any cytotoxic effects of nicotine (data not shown). Rather than inducing cell death, the exposure of HDPCs to nicotine increases the amount of DNA in the cells, and this process may involve ERK1/2. Although it has been suggested that the ERK pathway may be involved in mineralization or osteoblast differentiation both positively (35) and negatively (36), the present study suggests that signaling via the ERK pathway induced by nicotine negatively regulates the mineralization of HDPCs.

In summary, we show that nicotine inhibits the differentiation and mineralization of HDPC in vitro, probably via nAChRs. Our results suggest that the functions of dentin matrix synthesis and mineralization are decreased in the HDPC of smokers.

References

1. Carbone D. Smoking and cancer. Am J Med 1992;93:138–7.
2. Heeschen C, Jang JJ, Weis M, et al. Nicotine stimulates angiogenesis and promotes tumor growth and atherosclerosis. Nat Med 2001;7:833–9.
3. Ryder MI. The influence of smoking on host responses in periodontal infections. Periodontol 2000 2007;43:267–77.
4. Conti-Tronconi BM, McLane KE, Raftery MA, Grando SA, Protti MP. The nicotinic acetylcholine receptor: structure and autoimmune pathology. Crit Rev Biochem Mol Biol 1994;29:69–123.
5. Maus AD, Pereira EF, Karachunski PI, et al. Human and rodent bronchial epithelial cells express functional nicotinic acetylcholine receptors. Mol Pharmacol 1998; 54:779–88.
6. Arredondo J, Hall LL, Ndoye A, et al. Central role of fibroblast alpha3 nicotinic acetylcholine receptor in mediating cutaneous effects of nicotine. Lab Invest 2003;83:207–25.
7. Kawashima K, Fujii T. Extraneuronal cholinergic system in lymphocytes. Pharmacol Ther 2000;86:29–48.
8. Wang H, Yu M, Ochani M, et al. Nicotinic acetylcholine receptor alpha7 subunit is an essential regulator of inflammation. Nature 2003;421:384–8.
9. Gronthos S, Mankani M, Brahim J, Robey PG, Shi S. Postnatal human dental pulp stem cells (DPSCs) in vitro and in vivo. Proc Natl Acad Sci U S A 2000;97:13625–650.
10. Seux D, Couble ML, Hartmann DJ, Gauthier JP, Magloire H. Odontoblast-like cytodifferentiation of human dental pulp cells in vitro in the presence of a calcium hydroxide-containing cement. Arch Oral Biol 1991;36:117–28.
11. Durand SH, Flacher V, Romeas A, et al. Lipoteichoic acid increases TLR and functional chemokine expression while reducing dentin formation in in vitro differentiated human odontoblasts. J Immunol 2006;176:2880–7.
12. Pocock NA, Eisman JA, Kelly PJ, Sambrook PN, Yeates MG. Effects of tobacco use on axial and appendicular bone mineral density. Bone 1989;10:329–31.
13. Hollinger JO, Schmitt JM, Hwang K, Soleymani P, Buck D. Impact of nicotine on bone healing. J Biomed Mater Res 1999;45:294–301.

14. Fang MA, Frost PJ, Iida-Klein A, Hahn TJ. Effects of nicotine on cellular function in UMR 106-01 osteoblast-like cells. Bone 1991;12:283–6.
15. Kanter AR, El-Ghorab N, Marzec N, Margarone JE 3rd, Dziak R. Nicotine induced proliferation and cytokine release in osteoblastic cells. Int J Mol Med 2006;17:121–7.
16. Shimabukuro Y, Ueda M, Ichikawa T, et al. Fibroblast growth factor-2 stimulates hyaluronan production by human dental pulp cells. J Endod 2005;31:805–8.
17. Yamagita M, Shimabukuro Y, Nozaki T, et al. IL-15 up-regulates iNOS expression and NO production by gingival epithelial cells. Biochem Biophys Res Commun 2002;297:329–34.
18. Sato KZ, Fujii T, Watanabe Y, et al. Diversity of mRNA expression for muscarinic acetylcholine receptor subtypes and neuronal nicotinic acetylcholine receptor subunits in human mononuclear leukocytes and leukemic cell lines. Neurosci Lett 1999;266:17–20.
19. Mihovilovic M, Roses AD. Expression of alpha-3, alpha-5, and beta-4 neuronal acetylcholine receptor subunit transcripts in normal and myasthenia gravis thymus. Identification of thymocytes expressing the alpha-3 transcripts. J Immunol 1993;151:6517–24.
20. Wakkach A, Guyon T, Briand C, Tzavios S, Cohen-Kaminsky S, Berrih-Aknin S. Expression of acetylcholine receptor genes in human thymic epithelial cells: implications for myasthenia gravis. J Immunol 1996;157:3752–60.
21. Yamaguchi H, Friedman H, Yamamoto Y. Involvement of nicotinic acetylcholine receptors in controlling Chlamydia pneumoniae growth in epithelial HEp-2 cells. Infect Immun 2003;71:3645–7.
22. Bessey OA, Lowry OH, Brock MJ. A method for the rapid determination of alkaline phosphatase with five cubic millimeters of serum. J Biol Chem 1946;164:321–9.
23. Dahl LK. A simple and sensitive histochemical method for calcium. Proc Soc Exp Biol Med 1952;80:474–9.
24. Walker LM, Preston MR, Magnay JL, Thomas PB, El Haj AJ. Nicotine regulation of c-fos and osteopontin expression in human-derived osteoblast-like cells and human trabecular bone organ culture. Bone 2001;28:603–8.
25. Chang YC, Tsai CH, Yang SH, Liu CM, Chou MY. Induction of cyclooxygenase-2 mRNA and protein expression in human gingival fibroblasts stimulated with nicotine. J Periodontal Res 2003;38:496–501.
26. Carlisle DL, Liu X, Hopkins TM, Swick MC, Dhir R, Siegfried JM. Nicotine activates cell-signaling pathways through muscle-type and neuronal nicotinic acetylcholine receptors in non-small cell lung cancer cells. Pulm Pharmacol Ther 2007;20:629–41.
27. Moses KD, Butler WT, Qin C. Immunohistochemical study of small integrin-binding ligand, N-linked glycoproteins in reactionary dentin of rat molars at different ages. Eur J Oral Sci 2006;114:216–22.
28. Tanaka H, Tanabe N, Suzuki N, et al. Nicotine affects mineralized nodule formation by the human osteosarcoma cell line Saos-2. Life Sci 2005;77:2273–84.
29. Chang YC, Hume EM, Tai KW, Yang LC, Chou MY. Mechanisms of cytotoxicity of nicotine in human periodontal ligament fibroblast cultures in vitro. J Periodontal Res 2002;37:279–85.
30. Feyerabend C, Hegenbottam T, Russell MA. Nicotine concentrations in urine and saliva of smokers and non-smokers. Br Med J (Clin Res Ed) 1982;284:1002–4.
31. Stavropoulos A, Nyman S, Herrero F, Karring T. Smoking affects the outcome of guided tissue regeneration with bioresorbable membranes: a retrospective analysis of intrabony defects. J Clin Periodontol 2004;31:945–50.
32. Doyle SL, Hodges JS, Pesun IJ, Baesden MA, Bowles WR. Factors affecting outcomes for single-tooth implants and endodontic restorations. J Endod 2007;33:599–602.
33. Russell MA, Jarvis M, Iyer R, Feyerabend C. Relation of nicotine yield of cigarettes to blood nicotine concentrations in smokers. Br Med J 1980;280:972–6.
34. Arredondo J, Chernyavsky AI, Jolkovsky DL, Pinkerton KE, Grando SA. Receptor-mediated tobacco toxicity: cooperation of the Ras/Raf-1/MEK1/ERK and JAK-2/STAT-3 pathways downstream of alpha7 nicotinic receptor in oral keratinocytes. FASEB J 2006;20:2093–101.
35. Jaiswal RK, Jaiswal N, Bruder SP, Mbalaviele G, Marshak DR, Pittenger MF. Adult human mesenchymal stem cell differentiation to the osteogenic or adipogenic lineage is regulated by mitogen-activated protein kinase. J Biol Chem 2000;275:9645–52.
36. Nakayama K, Tamura Y, Suzuva M, et al. Receptor tyrosine kinases inhibit bone morphogenetic protein-Smad responsive promoter activity and differentiation of murine MC3T3-E1 osteoblast-like cells. J Bone Miner Res 2003;18:827–35.

歯根膜の分子基盤研究

山田　聡*　村上伸也*

歯を支える歯周組織のなかでも，とくに重要で特殊な機能を有する歯根膜の分子基盤を解明する目的で，ヒト歯根膜 3' 末端 cDNA ライブラリ解析をもとにして，ヒトの *in vivo* 歯根膜においていかなる遺伝子がいかなる頻度で発現しているのかを示すヒト歯根膜遺伝子発現プロファイルを作成した．その結果，歯根膜の特徴的な機能・形態を分子・遺伝子レベルで明らかにすることができた．さらに，歯根膜に特異的に発現している細胞外基質蛋白 PLAP-1 を見出した．発現・機能解析の結果，PLAP-1 は，硬組織形成に対して抑制的に作用することにより，硬組織形成能を有しながらも石灰化せず，線維性の結合組織として機能する歯根膜の恒常性を維持している可能性が示された．

はじめに

ヒトゲノムプロジェクト完了の結果，ヒトの全ゲノム配列が解読され，その遺伝子総数は 2 万 2 千個前後であることが明らかとなった．生命科学は，ポストゲノム時代に突入し，DNA からヒトへという新しい研究アプローチがなされつつある．われわれはこれまでに，歯周組織のなかでも，歯周組織の恒常性維持および歯周病によって破壊された歯周組織の修復・再生に中心的な役割を果たしている歯根膜に着目し研究をおこなっている．本稿では，そのなかの 1 つとして歯根膜研究の新しいアプローチを紹介したい．

〔キーワード〕
歯根膜
ポストゲノムサイエンス
3' 末端 cDNA ライブラリ
歯根膜遺伝子発現プロファイル
歯根膜特異的分子 PLAP-1

* YAMADA Satoru, MURAKAMI Shinya/大阪大学大学院歯学研究科口腔分子免疫制御学講座 歯周病分子病態学 歯周病診断制御学

1．ポストゲノムサイエンスとしての歯根膜研究

ヒトの歯根膜は，歯と歯槽骨という 2 つの硬組織の間に存在するコラーゲン線維に富む非石灰化の結合組織であり，線維性付着により歯を歯槽骨に保持するという役目を担いながら，咬合時の感覚受容器としても機能している．また，歯根膜は，100～250 μm の幅を保ちながら，咬合力，矯正力といったメカニカルストレスに反応して歯槽骨，セメント質および結合組織のリモデリングをおこない，歯周組織の動的平衡を保っていると考えられている．近年の研究から歯根膜は，石灰化関連分子やサイトカインを自ら産生することにより歯周組織の再生をもたらすこと，また，歯根膜組織は歯周組織の再生を可能ならしめる未分化間葉系細胞群のリザーバーとなっている重要な組織であることなどが明らかとなっている[1]．また，歯根膜由来の培養細胞を用いた数々の研究により，歯根膜由来の線維芽細胞は歯肉由来の線維芽細胞と比較して高い石灰化能を有し，硬組織形成に関与

する分子群の発現が高いことも明らかにされている[2]．この重要かつユニークな組織である歯根膜において，これまで形態的・機能的な特徴についての研究が中心になされてきが，遺伝子・分子レベルでの特徴については十分解析されたとはいいがたい．

ポストゲノムサイエンスとして，ヒト身体の各組織・細胞における特有の遺伝子発現パターンを大規模・網羅的に解析することにより，各々の組織・細胞における遺伝子発現の組み合わせを解明し，分子生物学的な側面からその組織・細胞の特徴や特有の機能を明らかにしようとする組織遺伝子発現プロファイル解析がおこなわれている．その1つとして，解析したい組織・細胞から3' 末端cDNAライブラリを構築するOkuboら[3]の方法が挙げられる．この3' 末端cDNAライブラリは，各cDNAクローンのインサートサイズが，3' 末端のpoly Aから上流の最初のMboIサイトまでの平均250塩基対となっており，逆転写酵素の効率やクローニング効率といったさまざまな二次的な影響を受けにくいことが特徴となっている．したがって，ライブラリ中のcDNAクローンの存在比率は，ソースとなった組織・細胞でのmRNA構成を正確に再現しているものと考えられる．このライブラリから無作為にクローンを抜き取り解析することにより，実際の組織・細胞における構成遺伝子の割合を正確に再現した「絶対的な」遺伝子発現量を示すプロファイリングが可能となる．さらに，同様の手法を用いて作成された身体各組織・細胞の遺伝子発現プロファイルデータを集積しデータベース化することにより(BodyMapプロジェクト)，各組織・細胞の遺伝子発現プロファイルをBodyMapデータベース上で比較検討し，組織・細胞特異的な遺伝子発現パターンを捉え，さらには特異的に発現する遺伝子を単離・同定することを可能にしている．そこで，われわれは，この手法を用いて歯根膜における遺伝子発現プロファイル解析(歯根膜のBodyMap)をおこなうことを試みた．

2．歯根膜の遺伝子発現プロファイル解析

われわれ[4]は，インフォームドコンセントが得られた矯正治療中の患者から治療のため便宜抜去された歯の歯根膜よりmRNAを抽出し，Okuboらの方法に従って歯根膜由来3' 末端cDNAライブラリを構築した(**図1**)．前述のように，このライブラリ中のcDNAクローンの存在比率は*in vivo*歯根膜での恒常的なmRNA構成を正確に再現しているものと考えられる．そこで，無作為に選択した1752個のcDNAクローンの塩基配列をDNAシークエンサーにて解読し，コンピューター解析による出現頻度および遺伝子バンクへの相同性検索をおこない，ヒト歯根膜遺伝子発現プロファイルを作成した(頻度7以上を**表1**に示す)．

歯根膜はコラーゲン線維に富んだ結合組織であり，そのコラーゲン線維を構成する主要な成分はⅠ型およびⅢ型コラーゲンである．ヒト歯根膜遺伝子発現プロファイル解析の結果，*collagen type* Ⅰ *alpha-2*，*collagen type* Ⅰ *alpha-1* および *collagen type* Ⅲ *alpha-1* 遺伝子の高発現を認め，歯根膜組織の特徴を遺伝子発現の側面からも裏付けた．また，*ribosomal protein* 遺伝子の高い発現を認めており，歯根膜組織ではコラーゲンの生合成がさかんにおこなわれ，結合組織のリモデリングが恒常的になされていることが推測される．ついで高い発現を認める *osteonectin* 遺伝子のコードする蛋白は，骨において豊富にみられる非コラーゲン性の基質蛋白であり，骨芽細胞から分泌され，マウス骨芽細胞様細胞MC3T3-E1を用いた系において石灰化ノジュールの形成にあわせてその発現が上昇するとの報告がある[5]．また，歯根膜細胞においては，osteonectin蛋白の発現上昇がmatrix metalloproteinases(MMPs)の産生を亢進させることにより，MMPsが細胞外基質を分解し，細胞外の微小環境を変化させ，歯根膜細胞の増殖を促進していると考えられている[6]．これらの知

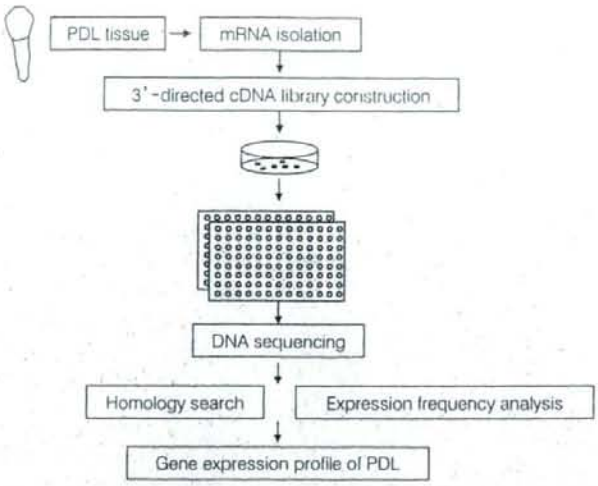

図 1. ヒト歯根膜遺伝子発現プロファイル解析

表 1. ヒト歯根膜遺伝子発現プロファイル

遺伝子名	発現頻度
collagen type Ⅰ alpha-2	63
collagen type Ⅲ alpha-1	47
collagen type Ⅰ alpha-1	45
osteonectin	22
ribosomal protein L21	12
periostin	8
ribosomal protein S18	8
ribosomal protein L13a	7
unknown*(PLAP-1)*	7

見より osteonectin は歯根膜組織のリモデリングを調整すると同時に硬組織形成に関与する分子であると考えられる．さらに，*periostin* 遺伝子の高い発現も同時に認められた．*periostin* 遺伝子は MC3T3-E1 のライブラリより単離・同定された遺伝子であり，骨膜表面と歯根膜組織に局在し，骨芽細胞の前駆細胞を遊走させ，歯槽骨および歯根膜組織のリモデリングをおこなっていると考えられている[7]．この *osteonectin* および *periostin* 遺伝子の高発現は，ヒト歯根膜組織の硬組織形成能を裏付けるものと考えられる．ヒト歯根膜組織遺伝子発現プロファイル解析により，新陳代謝の活発な線維性結合組織でありながら高い硬組織形成能をもつ歯根膜の組織特異性を遺伝子発現状況の側面から忠実に再現することができた．

3．歯根膜特異的分子 PLAP-1

歯根膜組織遺伝子発現プロファイルのなかに，出現頻度7という高発現を示すにもかかわらず，遺伝子バンクにも登録されていないまったく未知の新規 3' 末端配列が発見された(**表 1**)．全長 cDNA クローニングの結果，この遺伝子は全長 2.5kbp で，382 アミノ酸をコードする新規の遺伝子であることが明らかとなった(**図 2A**)．われわれ[1]は，この遺伝子を *periodontal ligament associated protein-1(PLAP-1)* と命名し，予想される蛋白をプロテインデーターベースにて検索したところ，興味深いことに，骨の形成や形態維持に重要な役割を果たしている細胞外基質プロテオグリカンである Decorin および Biglycan に対して非常に高い相同性を有する分子であることが明らかとなった．一方，ヒトの身体を構成する各組織より作成した臓器別遺伝子発現プロファイルをデータベース化した東大医科研 BodyMap データベース

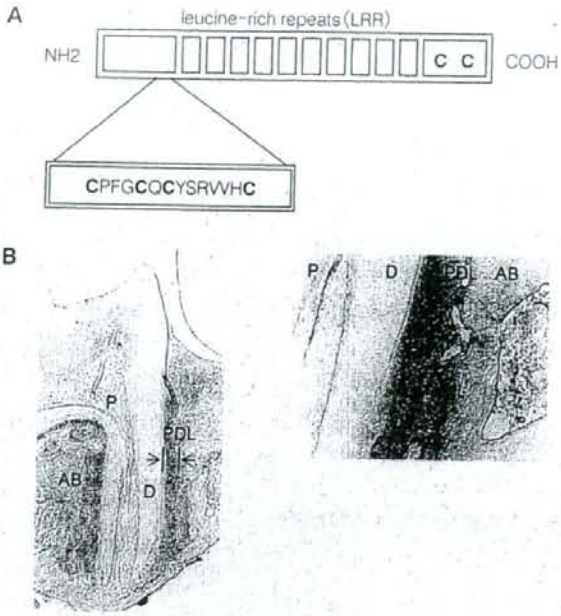

図 2. 歯根膜特異的細胞外基質 PLAP-1

A：PLAP-1 蛋白の構造

中央部に 10 個の LRR，N 末端および C 末端にシステインモチーフを有し，small leucine-rich repeat proteoglycan (SLRP) ファミリーに属する．

B：*in situ* ハイブリダイゼーション

(Yamada S *et al*, 2007[9] より改変引用)

マウス上顎歯周組織における *PLAP-1* 遺伝子の発現を解析した．左倍率 50 倍，右倍率 200 倍．AB：歯槽骨，D：象牙質，P：歯髄，PDL：歯根膜

を遺伝子検索した結果，*PLAP-1* 遺伝子は，わずか心臓結合組織および表皮乳頭状組織においてのみ，それぞれ一回の発現頻度でしか検出されなかった．これらの結果より，*PLAP-1* 遺伝子は歯根膜組織に特徴的に発現されており，その遺伝子産物である PLAP-1 蛋白は細胞外基質として，歯根膜における硬組織形成に関与している可能性が示唆された．

そこで，生体内における PLAP-1 の発現を解析するために，マウス歯周組織において *in situ* ハイブリダイゼションをおこなったところ，*PLAP-1* 遺伝子は，歯根膜に特異的に発現しており，歯肉や口腔上皮，歯槽骨，骨膜などにはまったくその発現が認められないことが明らかとなった(**図 2B**)．つぎに，硬組織形成を誘導した歯根膜細胞において *PLAP-1* 遺伝子の発現を解析したところ，硬組織形成に伴ってその遺伝子発現が亢進することが示された．さらに，各種増殖因子による *PLAP-1* 遺伝子発現への影響を検討したところ，骨形成誘導能をもつ BMP-2 および BMP-4 によって，PLAP-1 の発現が誘導され，塩基性線維芽細胞増殖因子 (FGF-2) 添加により *PLAP-1* 遺伝子の発現が著明に抑制された[8]．すなわち *PLAP-1* 遺伝子は硬組織形成の過程でそれらサイトカインにより発現制御を受けている可能性が示唆された．

つぎに *in vitro* において PLAP-1 を歯根膜細胞に強発現させ，その分化過程に及ぼす影響を検討した．興味深いことに，歯根膜細胞において PLAP-1 を強発現させることにより ALPase 活性の上昇および石灰化ノジュール形成が抑制され，BMP-2 刺激によって誘導される ALPase 活性の上昇も抑制された．一方，RNAi により歯根膜細胞の内在性 *PLAP-1* 遺伝子発現を抑制したところ，PLAP-1 を強発現させた場合とは逆に，BMP-2 刺激によって誘導される ALPase 活性がより増強された．さらに，リコンビナント PLAP-1 蛋白と BMP-2 蛋白との免疫沈降実験から，PLAP-1 と BMP-2 は直接結合することが明らかとなり，PLAP-1 は，歯根膜細胞の硬組織形成細胞への分化および硬組織形成を負に制御する分子であることが示され，その作用機序の一部は，

BMP-2を細胞外でアンタゴナイズし，BMPシグナルを抑制することにより担われている可能性が示唆された[9]．

以上から，歯根膜特異的分子であるPLAP-1は，硬組織形成に対して抑制的に作用することにより，硬組織形成能を有しながらも石灰化せず，線維性の結合組織として機能する歯根膜の恒常性を維持していることが示唆された．

おわりに

歯周組織の恒常性維持および歯周組織の再生・修復において中心的な役割を果たしている歯根膜について，われわれがこれまでに進めてきたトランスクリプトーム解析を中心とした研究をご紹介した．興味深いことに，他の複数の研究グループが，われわれと同時期に相次いで*PLAP-1*と同一の遺伝子を心臓または膝軟骨からクローニングし，*asporin*と名付けている[10][11]．最近，*asporin*が変形性関節症の原因遺伝子であり，TGF-βの作用を阻害することにより関節軟骨の再生・修復を制御していることも明らかとなっている[12]．関節軟骨は，細胞外基質が豊富で関節に加わるメカニカルストレスを緩和するクッションとしての機能も有し，歯根膜との形態的・機能的な類似性が高い組織と思われることから，PLAP-1/asporinが，歯根膜あるいは関節軟骨といった特殊な組織において，組織恒常性の維持や再生・修復の中心的な役割を果たしている重要な因子の1つであることが示唆される．現在，歯周病とPLAP-1/asporinとの関連性について解析をはじめており，その臨床研究の成果が待たれるところである．

文　献

1) Seo BM *et al*: Investigation of multipotent postnatal stem cells from human periodontal ligament. *Lancet* **364**: 149-155, 2004
2) Somerman M *et al*: A comparative study of human periodontal ligament cells and gingival fibroblast *in vitro*. *J Dent Res* **67**: 66-70, 1988
3) Okubo K *et al*: Large scale cDNA sequencing for analysis of quantitative and qualitative aspects of gene expression. *Nat Genet* **2**: 173-179, 1992
4) Yamada S *et al*: Expression profile of active genes in human periodontal ligament and isolation of PLAP-1, a novel SLRP family gene. *Gene* **275**: 279-286, 2001
5) Kelm R *et al*: Osteonectin in matrix remodeling. A plasminogen-osteonectin-collagen complex. *J Biol Chem* **269**: 30147-30153, 1994
6) Fujita T *et al*: Effects of transforming growth factor-beta 1 and fibronectin on SPARC expression in cultures of human periodontal ligament cells. *Cell Biol Int* **26**: 1065-1072, 2002
7) Wilde J *et al*: The divergent expression of periostin mRNA in the periodontal ligament during experimental tooth movement. *Cell Tissue Res* **312**: 345-351, 2003
8) Yamada S *et al*: Regulation of PLAP-1 expression in periodontal ligament cells. *J Dent Res* **85**: 447-451, 2006
9) Yamada S *et al*: PLAP-1/asporin: a novel negative regulator of periodontal ligament mineralization. *J Biol Chem* **282**: 23070-80, 2007
10) Henry SP *et al*: Expression pattern and gene characterization of asporin, a newly discovered member of the leucine-rich repeat protein family. *J Biol Chem* **276**: 12212-12221, 2001
11) Lorenzo P *et al*: Identification and characterization of asporin, a novel member of the leucine-rich repeat protein family closely related to decorin and biglycan. *J Biol Chem* **276**: 12201-12211, 2001
12) Kizawa H *et al*: An aspartic acid repeat polymorphism in asporin inhibits chondrogenesis and increase susceptibility to osteoarthritis. *Nature Genet* **37**: 138-144, 2005

再生医学のいま
―― 基礎研究から臨床への展開に向けて ――
16

歯周組織再生の現状と将来の展望

村上伸也* 橋川智子
大阪大学大学院歯学研究科歯周病分子病態学・歯周病診断制御学 准教授

Summary

歯周病は，歯を支えている歯周組織が慢性炎症的に破壊されていく疾患である．近年，歯根周囲の靱帯組織（歯根膜）に未分化間葉系幹細胞が成人になってもリザーブされていることが明らかにされ，同細胞を種々の方法で活性化することにより，失われた歯周組織を再生しようとする試みがなされている．GTR法やエナメルマトリクスタンパクを用いた既存の治療法に加えて，FGF-2などのサイトカインの局所投与や脂肪組織由来幹細胞の移入により，歯周組織再生誘導を図ろうとする臨床研究が推進されている．

I 歯周組織再生療法の現状

1 歯周病と歯周組織再生療法

われわれの歯は，2種類の硬組織（セメント質，歯槽骨）と2種類の軟組織（歯肉，歯根膜）からなる歯周組織により，顎骨に強固に支持されている．歯周病は細菌バイオフィルム（プラーク）に起因する感染症であり，疾患の進行に伴い，歯の支持組織である歯周組織が慢性炎症的に破壊される（図1）．歯周病は成人が歯を失う最大の原因であり，成人の約80%が罹患している「口」の生活習慣病としても位置づけられている．歯周治療の原則は，原因である細菌バイオフィルムを歯根表面の壊死セメント質とともに機械的に除去することであるが，それだけでは創傷治癒の場にいち早く到達する歯肉上皮により治癒が完了してしまい，セメント質や歯槽骨の新生を伴った真の歯周組織再生は望めない．したがって，中高年者，高齢者のQOLの維持・増進を考えたとき，予知性の高い新規歯周組織再生療法の開発は社会的急務であるといえる．

これまでの研究成果より，歯根周囲の靱帯組織である歯根膜組織のなかに骨芽細胞やセメント芽細胞へ分化し得る間葉系幹細胞が成人になっても存在することが示され[1]，歯根膜に存在するこのような細胞の機能を十分に発揮させる工夫をすることにより，従来の歯周治療では不可能と考えられてきた歯周組織の再生を誘導することが歯科医学的に可能であると現在では考えられている（図2）．

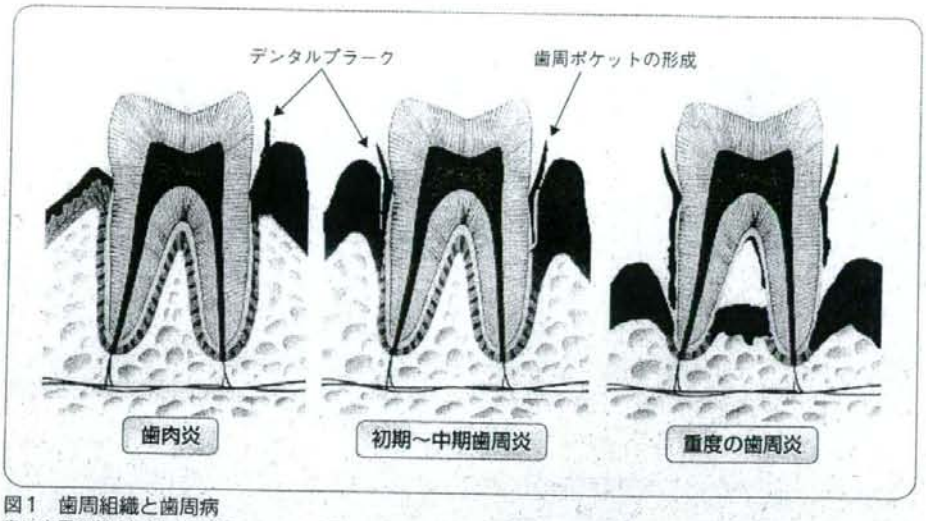

図1　歯周組織と歯周病
歯は歯周組織（歯肉・歯根膜・セメント質・歯槽骨）により顎骨に支持されている．そして歯周病は，デンタルプラーク中の細菌の影響により歯周組織が慢性炎症的に破壊されてゆく疾患である．

ここでいう歯周組織の再生というのは，①歯周組織欠損部に面する歯根面に歯根膜由来細胞が選択的，優先的に誘導され，②これら歯根膜由来細胞中に含まれる未分化間葉系幹細胞（歯周組織幹細胞）が分化能を保有したまま増殖し，硬組織形成細胞（骨芽細胞やセメント芽細胞）や歯根膜線維芽細胞として部位特異的な分化を遂げ，③歯根膜線維芽細胞によって産生されたコラーゲン線維束が骨芽細胞やセメント芽細胞により新生された骨組織，セメント質に埋入され歯と歯槽骨間に線維性の結合（いわゆる新付着）が再生されることを意味している．

2　歯周組織再生療法の現状

現在臨床応用されている歯周組織再生療法は，患歯の歯根膜組織に内在するいわゆる「歯周組織幹細胞」を幹細胞源に用いたものである．歴史の長いものとしては「骨移植」があげられる．これは患者の顎骨を一部採取・粉砕して得られた自家骨やアパタイトのような人工骨を歯周組織欠損部に充填することにより，同部の骨再生を促そうとするものである．1980年代に入り，「guided tissue regeneration（GTR）法」が臨床応用されるように

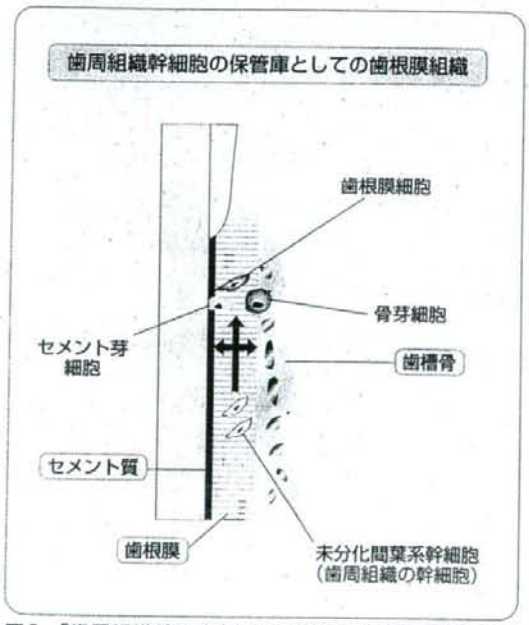

図2　「歯周組織幹細胞」としての未分化間葉系幹細胞が存在する歯根膜組織の概念図
歯根膜中にはセメント芽細胞，骨芽細胞，歯根膜細胞などへ分化する能力を保持しているいわゆる「歯周組織幹細胞」が，成人になっても存在している．